energies

MDPI

Article

A Surrogate Modeling Approach for Aggregated Flexibility Envelopes in Transmission–Distribution Coordination: A Case Study on Resilience

Marco Rossi *, Andrea Pitto, Emanuele Ciapessoni and Giacomo Viganò

Ricerca sul Sistema Energetico (RSE s.p.a.), Via Rubattino 54, 20134 Milano, Italy; andrea.pitto@rse-web.it (A.P.); emanuele.ciapessoni@rse-web.it (E.C.); giacomo.vigano@rse-web.it (G.V.)

* Correspondence: marco.rossi@rse-web.it

Abstract

The role of distributed energy resources in distribution networks is evolving to support system operation, facilitated by their participation in local flexibility markets. Future scenarios envision a significant share of low-power resources providing ancillary services to efficiently manage network congestions, offering a competitive alternative to conventional grid reinforcement. Additionally, the interaction between distribution and transmission systems enables the provision of flexibility services at higher voltage levels for various applications. In such cases, the aggregated flexibility of low-power resources is typically represented as a capability envelope at the interface between the distribution and transmission network, constructed by accounting for distribution grid constraints and subsequently communicated to the transmission system operator. This paper revisits this concept and introduces a novel approach for envelope construction. The proposed method is based on a surrogate model composed of a limited set of standard power flow components—loads, generators, and storage units—enhancing the integration of distribution network flexibility into transmission-level optimization frameworks. Notably, this advantage can potentially be achieved without significant modifications to the optimization tools currently available to grid operators. The effectiveness of the approach is demonstrated through a case study in which the adoption of distribution network surrogate models within a coordinated framework between transmission and distribution operators enables the provision of ancillary services for transmission resilience support. This results in improved resilience indicators and lower control action costs compared to conventional shedding schemes.

Keywords: surrogate model; resilience; TSO-DSO coordination; distribution network flexibility

check for updates

Academic Editor: Michael Negnevitsky

Received: 4 September 2025
Revised: 17 October 2025
Accepted: 18 October 2025
Published: 22 October 2025

Citation: Rossi, M.; Pitto, A.; Ciapessoni, E.; Viganò, G. A Surrogate Modeling Approach for Aggregated Flexibility Envelopes in Transmission–Distribution Coordination: A Case Study on Resilience. *Energies* **2025**, *18*, 5567. https://doi.org/10.3390/en18215567

Copyright: © 2025 by the authors. Licensee MDPI, Basel, Switzerland. This article is an open access article distributed under the terms and conditions of the Creative Commons Attribution (CC BY) license (https://creativecommons.org/licenses/by/4.0/).

1. Introduction

The continuous expansion of distributed generation and the electrification of loads, together with the development of storage systems, electric vehicles, and demand-side management technologies, are creating new opportunities for participation in energy, balancing, and ancillary service markets. These markets have traditionally been managed at the system level by the Transmission System Operator (TSO).

As a result, Distribution System Operators (DSOs) are required to actively manage their networks to provide a specified amount of local flexibility for transmission-level services [1–3]. In response, several research initiatives [4–6] and working groups [2,7,8] have advocated stronger TSO-DSO coordination, with the overarching goal of reducing total system planning and operational costs [9].

In principle, the most efficient strategy would be a unified optimization framework that jointly models both transmission and distribution systems. However, such an approach faces substantial challenges, including significant computational complexity [10,11] and, more critically, the lack of standardized and transparent protocols for data exchange between operators [7,12]. These limitations hinder the practical implementation of joint TSO-DSO optimization and underscore the need for incremental steps toward interoperable and coordinated operation.

A key enabler in this direction is the definition of standardized protocols and tools for the exchange of information between TSOs and DSOs, particularly regarding the flexibility potential of distribution networks [13]. To this end, the scientific community has proposed the concept of aggregated distribution flexibility, which provides a structured and privacy-preserving way to communicate available flexibility at the distribution level. This approach minimizes the amount of data exchanged while safeguarding both coordination effectiveness and the confidentiality of sensitive operational information.

1.1. Flexibility Capabilities and Optimization Challenges

Recent literature has extensively investigated the concept of flexibility capability, defined as the set of feasible operating points that distributed resources can provide under given constraints [13–20]. These capabilities are commonly represented through aggregated flexibility envelopes, which capture the collective behavior of distribution networks in terms of active and reactive power flexibility.

Such representations are useful for quantifying the contribution of distributed resources to system-level services. Nevertheless, flexibility envelopes often exhibit irregular shapes and time-varying characteristics, which are not directly compatible with the standard formulations used in Optimal Power Flow (OPF) models [21]. This limits their applicability in real-time coordination and market-based interactions between TSOs and DSOs.

1.2. Novelty and Contributions of This Work

To address this gap, this work introduces a surrogate modeling approach that represents the flexibility of the distribution network through a set of equivalent standard devices, such as generators, storage systems, and loads. These surrogate devices are constructed as combinations of regular, well-defined curves that emulate the aggregated behavior of the underlying distribution system while respecting network constraints (e.g., voltage and thermal limits).

The crucial feature of this approach is that the surrogate devices are directly compatible with conventional OPF models, allowing TSOs to incorporate distribution-level flexibility into their existing optimization and control frameworks without structural modifications. To the best of the authors' knowledge, no prior work has proposed a surrogate modeling framework based on standard elements explicitly designed for OPF compatibility. Existing studies have typically relied on simplified or reduced-order representations (e.g., irregular PQ-polygons), without systematically addressing the challenge of embedding aggregated flexibility into industrially available OPF tools.

Unlike previous approaches, the proposed methodology deliberately sacrifices a degree of modeling accuracy in favor of practical implementability and integration into SCADA-based optimization engines. The coordination process (Figure 1) unfolds as follows:

1. The DSO constructs the surrogate model, reserving part of the flexibility for local needs (e.g., voltage regulation, congestion management).
2. The equivalent surrogate model of residual flexibility is communicated to the TSO.
3. The TSO optimizes system operation based on the surrogate devices and transmits set-points to the DSO.

4. The DSO disaggregates these set-points and applies them to individual distributed resources (more specifically to the balancing/flexibility service providers).

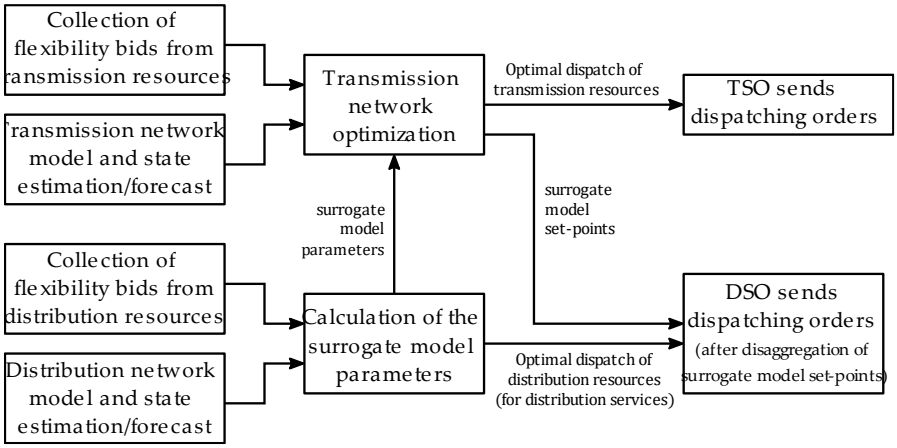


Figure 1. Flow diagram of a generic TSO-DSO coordination process, illustrating the information exchange between the main processes under the responsibility of system operators. It is important to note that the calculation of the optimal dispatch of distribution resources is embedded within the construction of the surrogate model.

Although this abstraction may result in a slight underutilization of the full flexibility potential, it substantially enhances the reliability, scalability, and interoperability of the coordination process. Importantly, this work extends previous efforts, focused primarily on active power flexibility [22], by explicitly incorporating reactive power flexibility as well, which is essential for maintaining voltage stability.

This extension represents a significant advancement, as it accounts for the inherently coupled nature of active and reactive power behavior in distribution networks. It is worth noting that [22] proposes an approach oriented towards TSO-DSO coordination in the planning phases of transmission and distribution networks. In contrast, the present manuscript focuses on operational coordination. Nevertheless, both processes rely on similar optimization tools and the same type of information exchange between system operators. Therefore, the coordination framework discussed here can be considered structurally equivalent to that proposed in [22].

The case study presented in this paper demonstrates how the proposed surrogate model can effectively capture distribution network flexibility and enable its integration into transmission-level resilience strategies, including modulation of the exchange profile at the primary substation and intentional islanding during contingencies.

1.3. Structure of the Manuscript

The remainder of the paper is organized as follows. Section 2 introduces the concept and role of the surrogate model within the context of TSO-DSO coordination. It presents the distribution network used as a reference for the analysis and details the step-by-step construction of each component of the surrogate model, including the abstraction of generators, storage systems, and controllable loads. This section lays the methodological foundation for the surrogate modeling approach proposed in this work. Section 3 evaluates the performance of the constructed surrogate model. It presents quantitative results that assess the model's ability to replicate the behavior of the original distribution network under various operating conditions, highlighting its accuracy and limitations. Section 4 shifts the focus to the transmission system to which the modeled distribution network is connected. This section introduces the case study designed to assess the impact of different contingency cases on system resilience. It analyzes how the flexibility provided by dis-

tributed resources (represented through the surrogate model) can contribute to mitigating the effects of transmission-level disruptions and support restoration procedures. Finally, Section 5 gathers the main conclusions of the analysis, highlighting that the surrogate model integrates effectively into transmission grid optimization procedures, as demonstrated by the results discussed in the previous sections.

2. Surrogate Model of Distribution Network

As previously mentioned, the surrogate model is designed as a simplified representation of the distribution network. It consists of a limited set of virtual devices that approximate the behavior of the actual network. These devices simulate both active and reactive power exchanges, as well as the flexibility associated with different categories of resources. To achieve this, the model employs lumped units, each of which aggregates the behavior of several physical devices connected to the network. These aggregated units share the same underlying model structure, although they may differ in specific parameters. This approach allows for a compact but representative abstraction of the system.

For example, consider a surrogate generator characterized by a rectangular active–reactive power capability curve. This single surrogate element can represent all generators within the network that exhibit rectangular capabilities. However, if other generators possess different capability shapes (such as triangular ones) a separate surrogate element must be introduced to capture their distinct behavior. The same principle applies when generators of the same type have different flexibility costs. In such cases, multiple surrogate units are needed to accurately reflect the techno-economic diversity of resources.

To illustrate the construction of such a surrogate model, we refer to the CIGRE medium-voltage distribution network benchmark [23], which is based on a real system located in Southern Germany, serving both a small town and its surrounding rural area. The benchmark is representative of typical MV networks found in both North America and Europe, although design philosophies and installation practices differ significantly between the two regions, a topic discussed in detail in [23]. The network topology (Figure 2a), connected devices, and time-dependent load and generation profiles are assumed to match those described in the same report. However, to create a more interesting case study (one that includes network congestion and the need for local flexibility services) some modifications are introduced. Specifically:

- The rated power of the wind generator at bus 7 is increased from 1.5 MW to 9 MW.
- The lines connecting bus 3 to bus 8, and bus 7 to bus 8 are reinforced.
- The existing storage units at bus 5 and bus 10 are exploited to mitigate local congestion caused by excess generation. These units have maximum active powers of 0.6 MW and 0.2 MW, capacities of 1.2 MWh and 0.4 MWh, respectively, and a round-trip efficiency of 81%.
- An additional storage unit with a capacity of 2 MWh and a maximum power of 1 MW is connected to bus 14, featuring a round-trip efficiency of 81% too.

In this modified network, all storage units are modeled with rectangular capability curves. Local generators are also assumed to follow rectangular capabilities, with a marginal cost of 5 amu/MWh for active power. Loads are considered curtailable, with a cost equal to the value of lost load, set at 5000 amu/MWh. The active power inflow from the transmission network is modeled with a cost of 100 amu/MWh.

As a result, the entire distribution network can be effectively represented by a surrogate model (Figure 2b) composed of just three elements which, according to the adopted economic merit order can be listed as:

- a lumped storage unit,
- a lumped generator,

- and a lumped load.

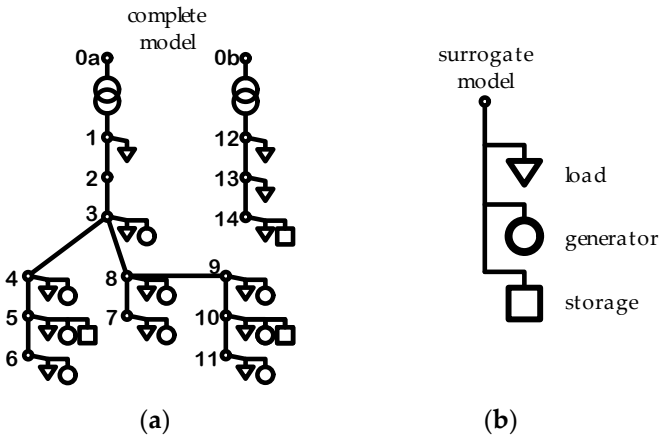


Figure 2. Single line diagram of the considered distribution network: (**a**) Complete model, with a detailed representation of each grid element and device; (**b**) Surrogate model, containing the surrogate storage unit, generator, and load.

This abstraction captures the essential techno-economic characteristics of the system while significantly reducing computational complexity.

The role of flexibility costs, especially in the presence of network bottlenecks, is fundamental when constructing the surrogate model. Grid constraints do not affect all resources equally [20]. For instance, when multiple resources are connected downstream of a line with limited transfer capacity, the system will naturally prioritize the cheapest flexibility options in case of congestion. These are dispatched first, while more expensive resources are only activated later (if the line capacity still allows it). As a result, the most expensive flexibility may be partially or entirely excluded due to upstream congestion. This behavior has a direct implication on how the surrogate model should be constructed: it must be built element by element, following the merit order of the available resources and the presence of possible grid bottlenecks. In other words, the surrogate model must reflect not only the technical capabilities of the components but also their economic dispatch priority. The procedure for constructing the surrogate model can be summarized in four main steps (Figure 3):

1. Solve the optimal local dispatch problem for the distribution network. This step identifies the optimal set-points for all flexible resources, aiming to resolve local congestion while minimizing the overall cost, including both local generation and power inflow from the transmission system.
2. Classify all components based on their techno-economic characteristics. This includes their capability curves (e.g., rectangular or triangular), internal constraints, and flexibility costs. Each category of components is then represented by a single lumped element in the surrogate model.
3. Establish a merit order within each category, ranking components by their flexibility cost. Following this order, the aggregate capability of each category is computed in terms of the active and reactive power that can be delivered to the transmission system via the primary substation.
4. Derive the parameters of each lumped element from the analysis of the aggregated capability curves. These parameters define the behavior of the surrogate model and ensure it accurately reflects the underlying network.

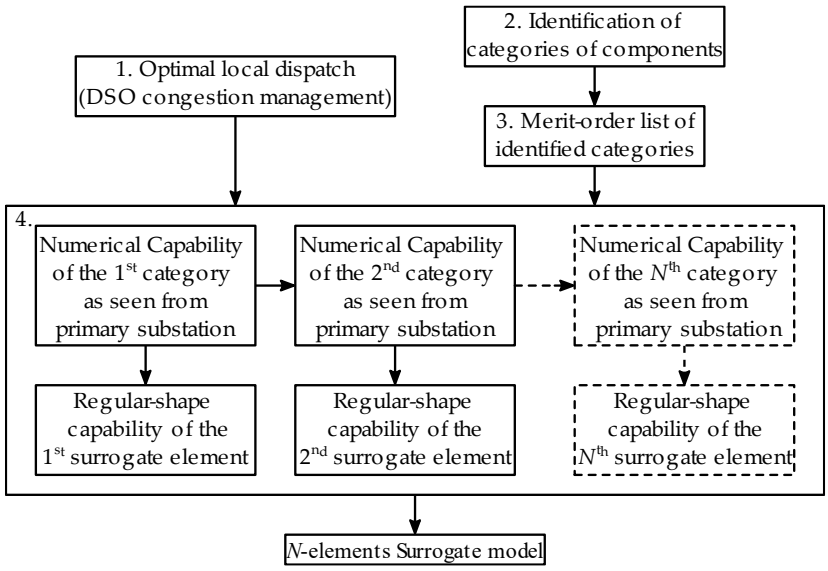


Figure 3. Flow diagram of the procedure to build the surrogate model.

Step 4 of the procedure is structured into two sub-steps. First, the numerical capability is computed, which can be obtained using any of the methods proposed in the literature and reviewed in [14–17]. Second, a suitable subset of this numerical capability is selected to match the regular capability curve required by the surrogate element. This second sub-step is described in detail in the following subsections. Although numerous techniques are available for the first sub-step, this work adopts the method presented in [24], which offers a good balance between accuracy and ease of integration into optimization tools currently used by system operators. As discussed in the introduction, it is important to note that the reconstruction of the (irregular) capability of aggregated distribution resources (approaches in [13–17,24]) constitutes only one component of the overall procedure and should not be interpreted as an alternative to the full modeling framework proposed in this study.

2.1. Distribution Network Baseline

The first step in constructing the surrogate model involves evaluating the baseline dispatch of flexible resources required to resolve local network congestions. This is achieved through an OPF analysis, which identifies the minimum set of actions necessary for the distribution system to operate within its technical limits. For the purposes of this discussion, we adopt the linear approximation described in [25], which efficiently determines the set-points of all flexible units involved in mitigating local constraints. These set-points are crucial, as they allow the calculation of the remaining flexibility margins (that is, the portion of flexibility that can still be offered to the transmission system). These margins are what the surrogate model ultimately aims to capture.

A key requirement for the surrogate model is that, when no flexibility is requested by the TSO, it must preserve the baseline power exchange (Figure 4) between the transmission and distribution networks. In other words, the surrogate model should behave identically to the real system under normal operating conditions, ensuring consistency and reliability.

Another critical consideration is the interaction between local and transmission-level services. Flexibility activated by the DSO to solve local issues can directly impact on the availability of flexibility for transmission services. For example, if a resource is dispatched downward by the DSO to alleviate local overloads, it cannot simultaneously provide upward flexibility to the TSO. Similarly, when a storage unit is used for local services, its state of charge is altered (Figure 5), which affects the volume of energy it can later offer to the transmission system.

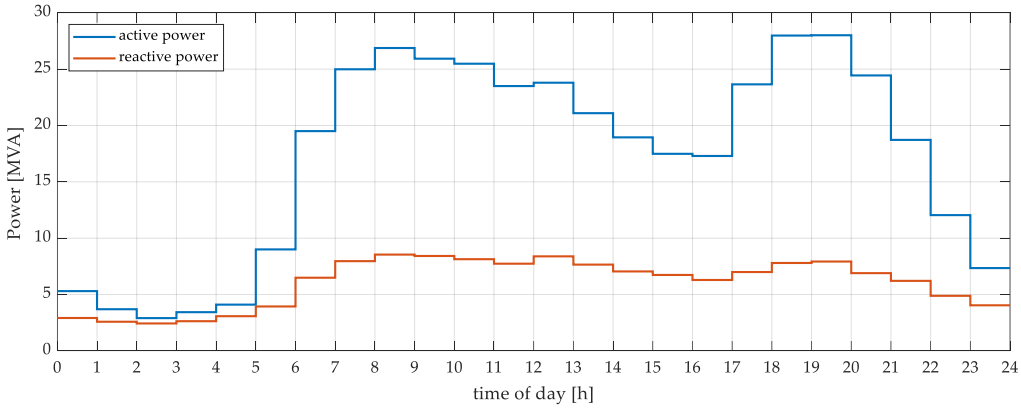


Figure 4. Total power exchange from transmission to distribution system.

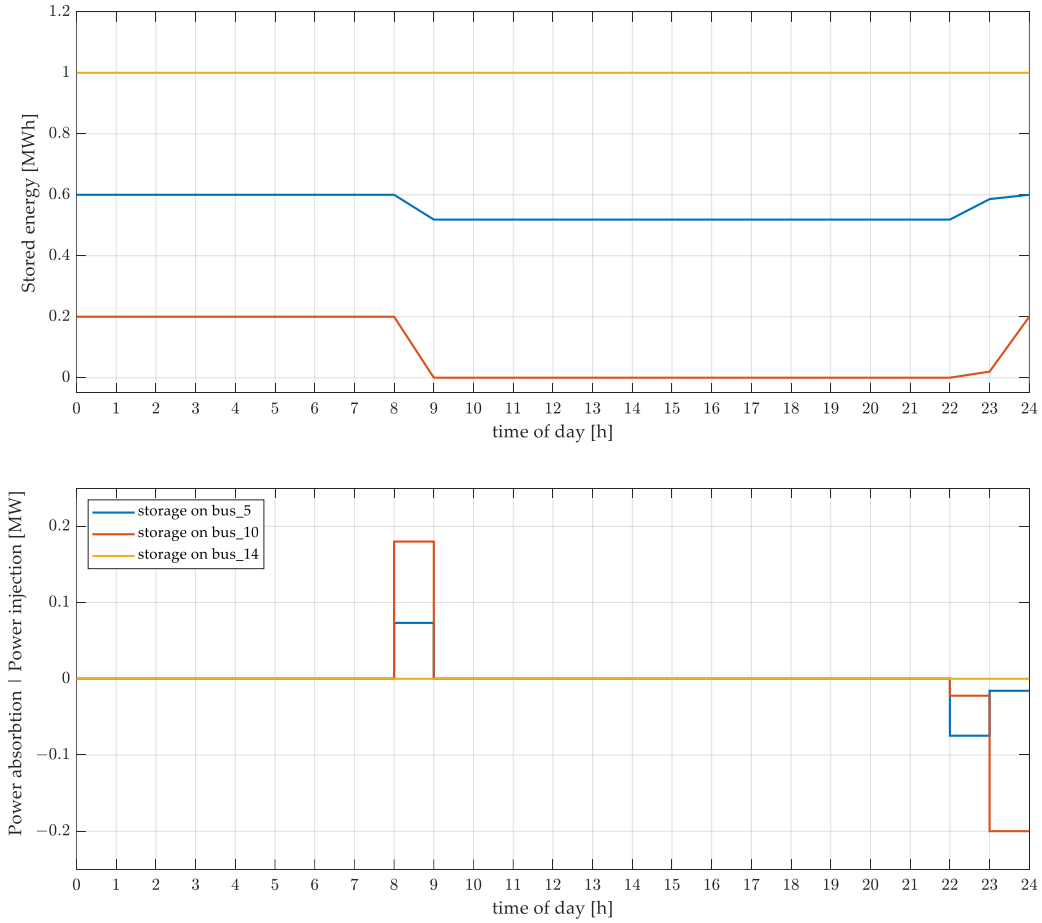


Figure 5. Energy and power profile of the storage units connected to distribution network.

These interdependencies must be carefully accounted for in the construction of the surrogate model. The model must reflect not only the technical capabilities and economic characteristics of each resource, but also the constraints imposed by prior activations and operational priorities. Only by incorporating these aspects can the surrogate model provide a realistic and useful representation of the potential of distribution network flexibility.

2.2. Model of the Surrogate Storage Unit

The first component in the merit order list is the lumped storage unit, which represents the aggregated behavior of all storage devices connected to the considered distribution network. Its characteristics are derived from the combination of individual storage units, ensuring that the surrogate model reflects their collective capability.

In the considered network, three storage units are present. When their capabilities are merged (without considering operational constraints) the resulting lumped device features a rectangular power capability of ± 1.8 MW and ± 1.8 Mvar, along with a total energy capacity of 2.6 MWh. These values are obtained by summing the individual contributions of each unit. Importantly, the round-trip efficiency of 81% is preserved in the surrogate model, ensuring consistency with the actual devices.

However, as discussed in Section 2.1, storage plays a critical role in managing local congestion. This means that, depending on the operational context, some storage units may be temporarily unavailable for transmission level services. Their flexibility might be inhibited due to prior commitments to local dispatch, which directly affects both their power availability and energy state. Consequently, the aggregated capability of the lumped storage unit is not static. The total stored energy and the volume of flexibility available for transmission services are influenced by how the storage is used locally. For example, if a unit is discharged to resolve a local issue, its ability to provide upward flexibility to the transmission system is reduced. To accurately capture these dynamics, a mathematical model of the lumped storage unit must be developed. This model should account for variations in power availability and accumulated energy, reflecting the interplay between local and transmission-level services. The formulation of such a model is presented in Equation (1), which integrates these operational dependencies into the surrogate representation:

$$E_S(t) = E_S(t - \Delta t) + \eta_{abs} \Delta t P_{Sabs}(t) - \frac{\Delta t}{\eta_{inj}} P_{Sinj}(t) + \Delta t P_{Sext}(t) \tag{1}$$

where for a specific time step t and time resolution Δt, E_S is the stored energy, P_{Sabs} is the active power absorbed from the grid and P_{Sinj} the power injected. In the implemented storage model, P_{Sabs} and P_{Sinj} are not mutually exclusive by design, meaning they can technically occur simultaneously. However, such simultaneous (non-physical) operation is penalized during optimization, as it leads to higher energy losses compared to models where they are temporally separated. If the risk of concurrent power flows is considered unacceptable (or if specific operating conditions require strict separation) these two variables can be encoded using special order constraints, ensuring mutual exclusivity within the optimization framework. Having verified this condition, the energy accumulation depends on the conversion efficiency, which is assumed to be η_{abs} during the power absorption phase, and η_{inj} when power is injected. The physical limitations of the storage units impose that:

$$\begin{cases} 0 \leq P_{Sabs}(t) \leq P_{Sabs}^{max}(t) & \text{active power absorbtion of storage} \\ 0 \leq P_{Sinj}(t) \leq P_{Sinj}^{max}(t) & \text{active power injection of storage} \\ E_S^{min} \leq E_S(t) \leq E_S^{max} & \text{stored energy} \end{cases} \tag{2}$$

The last quantity reported in (1) identifies the external-process power P_{Sext}. This term is sometimes included in classical OPF formulations to model external inflows of energy, such as those from natural basins feeding pumped hydro storage systems [26]. In the context of this study, P_{Sext} is used to account for the impact of local distribution dispatching on the stored energy of the lumped storage unit. It reflects how local operations (such as congestion management) can alter the energy state of the storage system, which influences its availability for transmission-level services.

Moreover, the model must also incorporate reactive power exchange, which is another flexibility service delivered by storage units. The reactive power exchanged by the lumped storage unit is expressed as:

$$Q_S(t) = Q_S^{base}(t) + \Delta Q_S(t) \tag{3}$$

where Q_S^{base} represents the baseline reactive power, while ΔQ_S identifies the deviation from this baseline, which occurs in case of flexibility activations for transmission services. Reactive power variation is subject to operational constraints, defined as:

$$\Delta Q_S^{min}(t) \leq \Delta Q_S(t) \leq \Delta Q_S^{max}(t) \tag{4}$$

To accurately capture the dynamics of distribution network flexibility, it is essential to recognize that all relevant quantities and constraints are time-dependent. Flexibility is not a static attribute since it evolves with the operational context, especially in systems where intertemporal constraints, such as energy storage, play a significant role. The procedure for reconstructing the aggregated storage capability is inspired by the methodology proposed in [22], which consists of three main steps:

1. Fix the dispatch of all flexible resources except storage: All non-storage flexible units are constrained to follow the power set-points determined by the optimal local dispatch (as described in Section 2.1). This ensures that their contribution to local congestion management is preserved and does not interfere with the analysis of storage flexibility.
2. Relax the intertemporal constraints of the storage model: While the structural model of the storage units is maintained, the energy balance constraints (which link power injection and absorption over time) are temporarily disabled. This allows the analysis to focus solely on the instantaneous power capability of the storage system, without being influenced by its current state of charge.
3. Numerically reconstruct the equivalent capability: Using one of the approaches described in literature (e.g., the one proposed in [24]), the aggregated capability of the lumped storage unit is computed at the point of common coupling between the transmission and distribution networks. This reconstruction returns a capability curve (as shown in Figure 6a), which reflects the maximum active and reactive power that the storage system can exchange at a given moment.

As illustrated in Figure 6a, the presence of network bottlenecks and the local dispatching of storage units can significantly alter the shape of the aggregated capability curve. The unconstrained capability (curve A) represents the theoretical maximum flexibility of the lumped storage unit, assuming no limitations from network constraints or prior dispatch decisions. However, in practice, these constraints lead to a distorted capability curve, shown by curve B. This curve reflects the actual flexibility available at the point of common coupling, after accounting for local congestion and the operational commitments of the storage units. The deviation from the ideal curve highlights the impact of grid limitations on the flexibility that can be offered to the transmission system. Moreover, since the lumped storage unit is modeled with a rectangular active/reactive power characteristic, the surrogate model must further simplify the capability curve to ensure representability. This involves inscribing a rectangle within the distorted curve B, such that the resulting surrogate capability (curve C) remains consistent with the model assumptions. Among the possible inscribed rectangles, the one that maximizes active power flexibility is selected. This choice ensures that the surrogate model prioritizes active power flexibility, while still respecting the constraints imposed by the network and local dispatch.

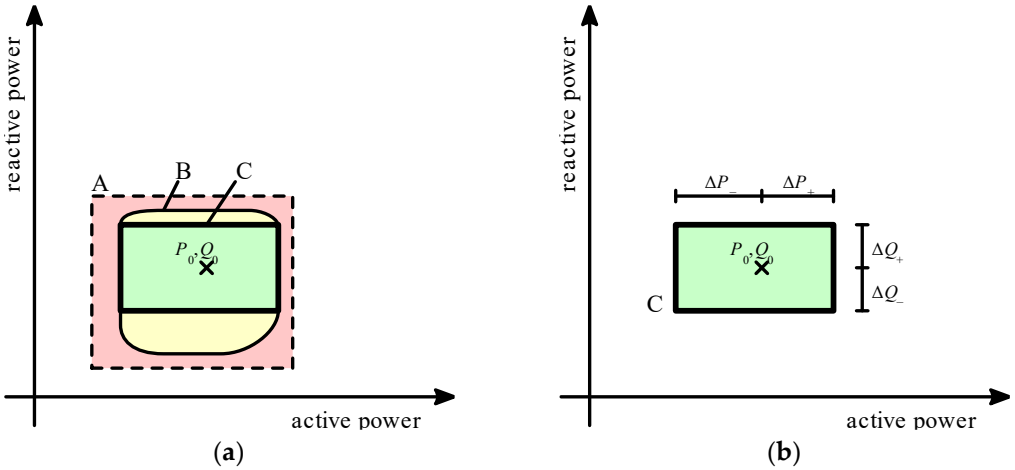


Figure 6. Equivalent capability of aggregated storage flexibility. P_0 and Q_0 (black cross) correspond to the active and reactive power exchange between distribution and transmission systems. In (**a**) Curve A illustrates the aggregated flexibility of all storage units without considering grid constraints. Curve B shows the aggregated flexibility after accounting for grid constraints. Curve C represents the capability curve of the surrogate storage element. (**b**) reports the details of curve C.

By referring to the quantities reported on Figure 6b, the parameters of the surrogate storage can be expressed as:

$$\begin{cases} P_{Sinj}^{max}(t) = \Delta P_+(t) & \text{maximum active power injection of storage} \\ P_{Sabs}^{max}(t) = \Delta P_-(t) & \text{maximum active power absorbtion of storage} \\ Q_S^{max}(t) = \Delta Q_+(t) & \text{maximum reactive power of storage} \\ Q_S^{min}(t) = \Delta Q_-(t) & \text{minimum reactibe power of storage} \end{cases} \tag{5}$$

The reactive power baseline Q_S^{base} can be selected arbitrarily and, for simplicity, it is assumed to be equal to zero. The resulting trends of the extracted quantities are illustrated in Figure 7, where periods of local congestion management involving storage can be identified by the occasional gaps in the maximum active power injection and absorption profiles. These interruptions indicate moments when the storage units are dispatched (dashed lines in Figure 7) by the DSO to resolve local issues. During these intervals, the upward and downward flexibility of the storage is limited. The same analysis can be extended to reactive power modulation, which capability is influenced by local network bottlenecks.

The dashed line in Figure 7 indicates the aggregated working point of all storage units connected to the distribution network. This point differs from the baseline of the surrogate model, as its effect on the power exchange between transmission and distribution is captured by the other surrogate elements (see next sections). However, its impact on the accumulated energy is explicitly considered through the external process power term. To consider the impact of local optimal dispatch and to accordingly limit the lumped storage flexibility, P_{Sext} is calculated by processing the results illustrated in Figure 5 by means of:

$$P_{Sext}(t) = \frac{1}{\Delta t} \sum_{\substack{\text{storage} \\ \text{units } k}} [E_k(t) - E_k(t - \Delta t)] \tag{6}$$

where E_k is the accumulated energy resulting from the solution of the optimal local dispatch problem for the k-th storage unit. Finally, the energy of the surrogate storage behaves as the combination of the ones of all the aggregated units (Figure 8).

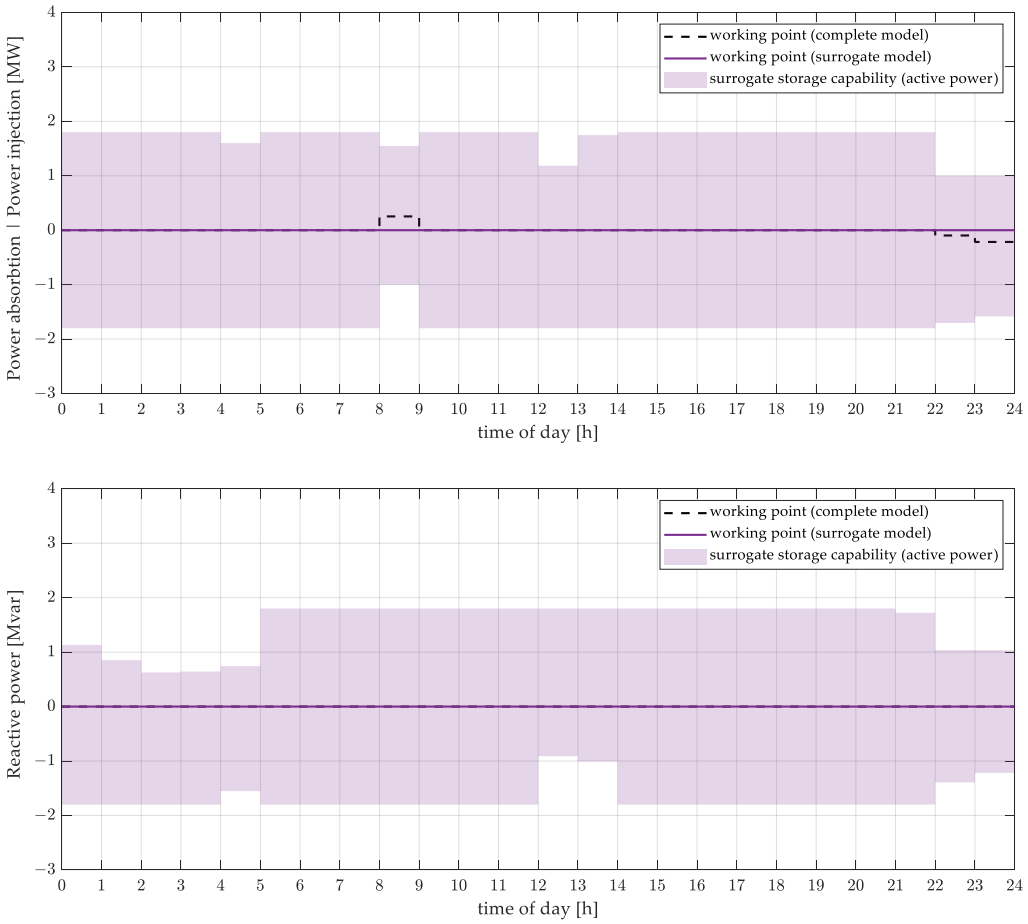


Figure 7. Time evolution of the power capability of the surrogate model for the storage (maximum power injection and absorption, maximum and minimum reactive power).

These insights further emphasize the importance of designing a surrogate model that accurately captures the time-dependent and asymmetric nature of flexibility availability, especially under realistic operating conditions. The final component in the modeling of the surrogate storage unit is the external process power P_{Sext}, which completes the representation of its behavior.

As discussed earlier, this term does not aim to cover all possible operating points of the individual storage units. Instead, it provides an efficient abstraction that includes the largest feasible capability area that can be represented by a single, simplified element, without violating the operational constraints of the distribution network.

2.3. Model of the Surrogate Generation Unit

Once the portion of flexibility associated with storage units has been extracted, the next step in the merit order list involves the generators. In the considered distribution network, generation units typically operate at their maximum available power under normal conditions. For the analyzed network, thanks to the support provided by local storage systems, no curtailment is required, which implies that these generators can only offer downward regulation as a flexibility service.

The procedure for constructing the aggregated capability of generators follows a similar approach to the one used for storage units (see Section 2.3), and consists of the following steps:

1. The intertemporal constraints of the storage units are removed, and their maximum injection/absorption limits are adjusted to match the capability determined in the

previous step. This ensures that the influence of storage active and reactive power on the network is properly considered.

2. The flexibility of all generators is enabled, allowing them to modulate their output power. Meanwhile, the load profiles are fixed to the values obtained from the optimal local dispatch, meaning that load curtailment is disabled during this phase.
3. The equivalent capability of the generators is then numerically reconstructed at the point of common coupling between the transmission and distribution networks. This reconstruction is carried out using the methodology described in [24], and an exemplificative capability curve is illustrated in Figure 9a.

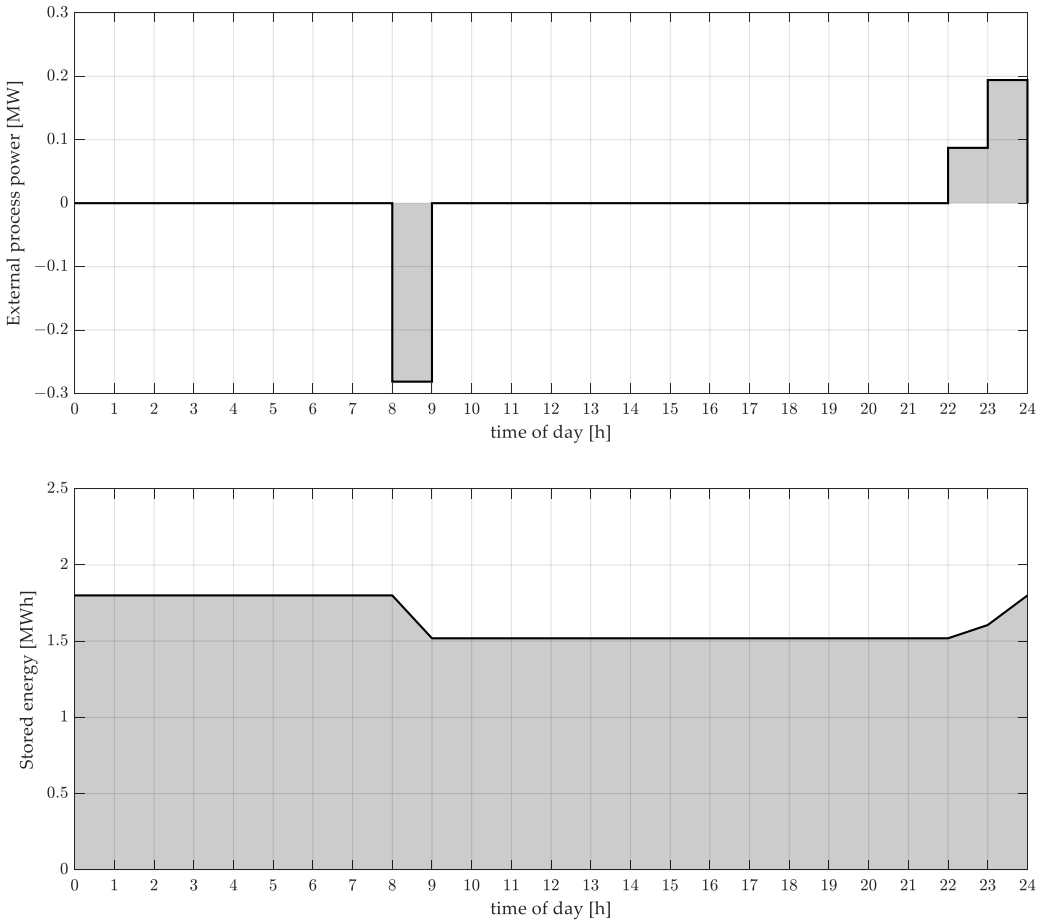


Figure 8. Time evolution of the baseline accumulated energy within the surrogate storage, resulting from the application of the computed external process power.

Also in this case the model of the surrogate generator resembles the one of the individual units, and the active/reactive power exchange can be formulated as:

$$\begin{cases} P_G(t) = P_G^{base}(t) + \Delta P_G(t) & \text{active power of generation} \\ Q_G(t) = Q_G^{base}(t) + \Delta Q_G(t) & \text{reactive power of generation} \end{cases} \tag{7}$$

where P_G^{base} and Q_G^{base} are the baseline active and reactive power contribution, while ΔP_G and ΔQ_G are the possible power variations which are optimization variables subject to the following constraints:

$$\begin{cases} \Delta P_G^{min}(t) \leq \Delta P_G(t) \leq \Delta P_G^{max}(t) & \text{active power variation of generation} \\ \Delta Q_G^{min}(t) \leq \Delta Q_G(t) \leq \Delta Q_G^{max}(t) & \text{reactive power variation of generation} \end{cases} \tag{8}$$

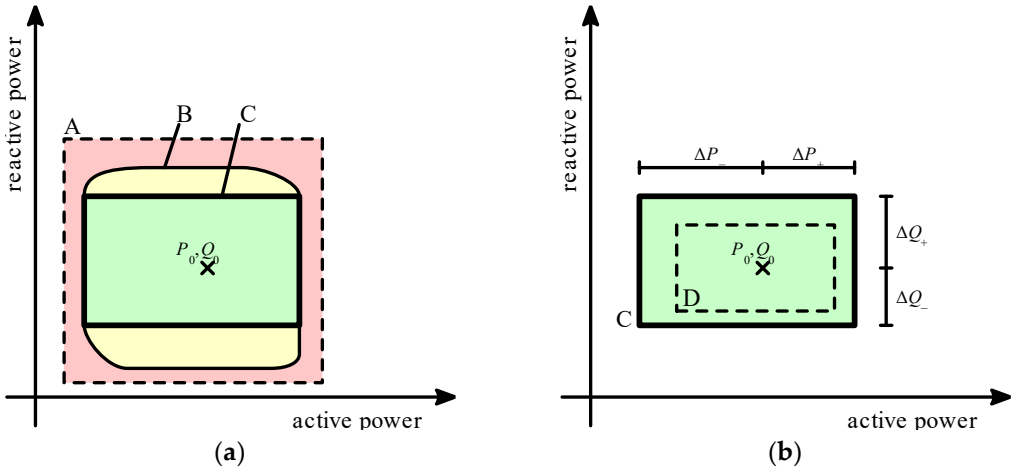


Figure 9. Equivalent capability of aggregated storage and generation flexibility. P_0 and Q_0 (black cross) correspond to the active and reactive power exchange between distribution and transmission systems. In (**a**) Curve A illustrates the aggregated flexibility of all storage and generation units without considering grid constraints. Curve B shows the aggregated flexibility after accounting for grid constraints. Curve C represents the combined capability curve of the surrogate storage and generation elements. (**b**) reports the details of Curve C, where Curve D indicates the portion of the total capability attributable to the surrogate storage.

As in the previous step, the final capability curve used to represent the behavior of the surrogate model is selected as the inscribed rectangle that maximizes active power flexibility, while still including the baseline operating point (see Figure 9a). In this case, the resulting capability (curve C) reflects the combined flexibility of both the surrogate storage unit (curve D) and surrogate generator (Figure 9b).

To isolate the contribution of the generator, the aggregated curve must be processed to extract the portion attributable specifically to generation. Fortunately, since both storage and generator capabilities are modeled as rectangular regions, this separation can be performed straightforwardly. The parameters of the surrogate generator are then derived by subtracting the storage rectangle (curve D) from the combined capability (curve C). This results in a new rectangular region that accurately represents the flexibility offered by the generators, consistent with the merit order and the operational constraints of the distribution network.

$$\begin{cases} \Delta P_G^{max}(t) \leq \Delta P_+(t) - P_{Sinj}^{max}(t) & \text{max.upward active power of generation} \\ \Delta P_G^{min}(t) \leq \Delta P_-(t) - P_{Sabs}^{max}(t) & \text{max.downward active power of generation} \\ \Delta Q_G^{max}(t) \leq \Delta Q_+(t) - \Delta Q_S^{max}(t) & \text{max.upward reactive power of generation} \\ \Delta Q_G^{min}(t) \leq \Delta Q_-(t) - \Delta Q_S^{min}(t) & \text{max.downward reactive power of generation} \end{cases} \quad (9)$$

The time evolution of the extracted quantities is illustrated in Figure 10, where it becomes evident that both active and reactive power exhibit time-varying profiles. This variability reflects the dynamic nature of the distribution network and its response to changing operating conditions.

Since the optimal dispatch of the distribution network converges to the maximum power injection from local generators, the flexibility available for transmission services is limited to downward regulation. In this context, the volume of downward active power flexibility corresponds to the aggregated output of local generators. However, while the volume of downward flexibility matches that of the complete model, the baseline operating point of the surrogate model differs. This discrepancy arises from the process of aligning the surrogate model capability with that of the full network. The selection of the baseline is

discussed in Section 2.4, as it must also account for the behavior of the surrogate load, which is optimized in that step. Nevertheless, Figure 10 anticipates the result. A similar analysis applies to reactive power, where the same modeling principles and constraints influence the surrogate representation. According to Section 2.2, the baseline is also influenced by the power exchanges of the considered storage units, which are not modeled within the surrogate storage unit except for its impact on the stored energy.

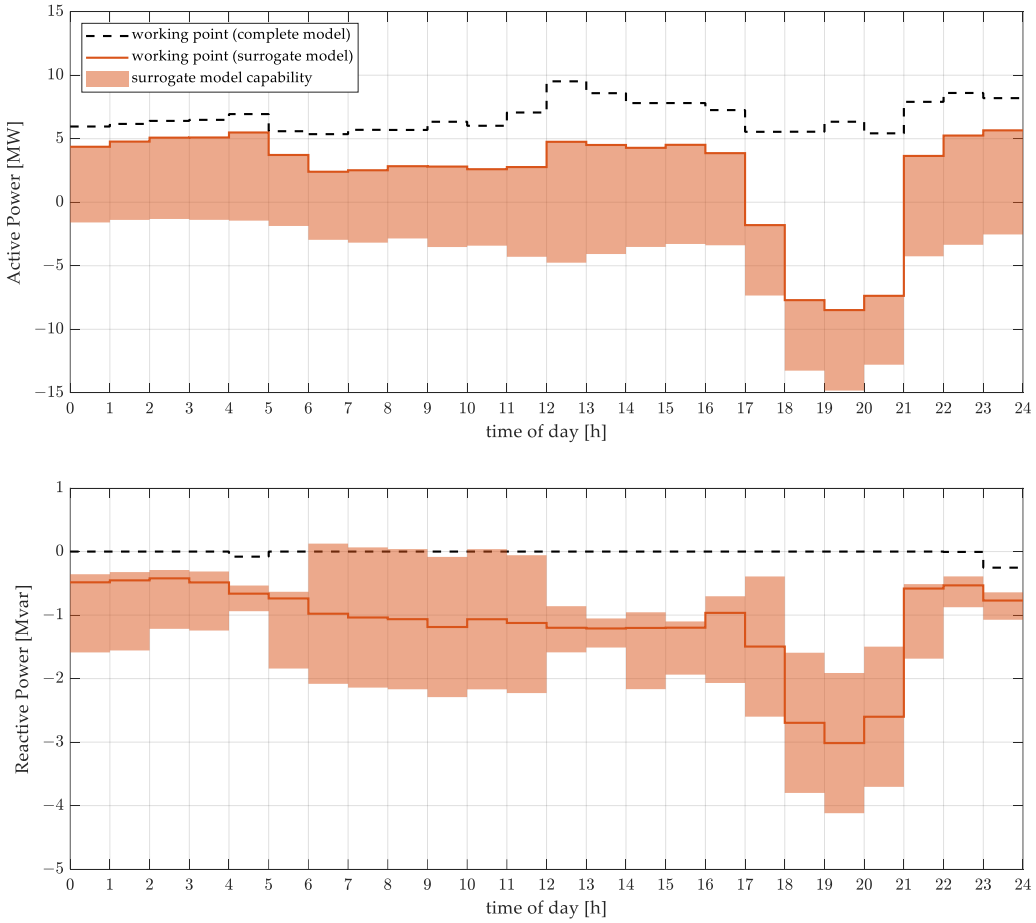


Figure 10. Time evolution of the power capability of the surrogate model for the generation (maximum and minimum active/reactive power variation with respect to the baseline).

As assumed, generation power has a lower flexibility activation priority compared to storage. This means that its flexibility is only utilized when the network capacity is not already occupied by storage dispatch. This prioritization reflects the merit order logic and ensures that the most cost-effective flexibility is used first.

2.4. Model of the Surrogate Load Unit

The final component to be included in the surrogate model is the lumped load. Under normal operating conditions, load units do not exhibit flexibility (unless they are part of demand-side management programs, which is not the case in this study). As a result, the load does not directly influence the shape of the capability curve. However, for studies focused on resilience, it is important to include the possibility of demand curtailment, which can be represented using a suitable mathematical formulation:

$$\begin{cases} P_L(t) = P_L^{base}(t) - P_L^{curt}(t) & \text{active power of load} \\ Q_L(t) = P_L(t)\tan(\varphi_L) & \text{reactive power of load} \end{cases} \quad (10)$$

where P_L is the actual active power consumption, which follows the base demand P_L^{base} and can be reduced by acting on the curtailment variable P_L^{curt}:

$$0 \leq P_L^{curt}(t) \leq P_L^{base}(t) \tag{11}$$

In terms of reactive power, the load is assumed to follow a fixed power factor angle φ_L, meaning that reactive power Q_L is proportional to active power. Ideally, this would require all load units to share the same active/reactive power ratio. While this condition is not strictly met in the distribution network under test, the deviation is considered acceptable for modeling purposes. Therefore, φ_L is calculated as the average power factor angle of the total demand. Once this parameter is defined, the capability curve of the lumped load can be constructed using the same procedure applied in previous steps:

1. The intertemporal constraints of storage units are removed, and their maximum injection/absorption limits are adjusted to match the capability obtained in the previous step.
2. The flexibility of all generators and load units is enabled, allowing for the simulation of demand curtailment.
3. The equivalent capability is then numerically reconstructed at the point of common coupling between the transmission and distribution networks, following the methodology described in [24].

Figure 11a illustrates how distribution network bottlenecks constrain the theoretical maximum flexibility (represented by curve A) to a smaller feasible area (curve B). This reduction reflects the impact of local constraints and dispatch priorities. Furthermore, when all components of the surrogate model are activated, the representable area is further limited to an inscribed hexagon, denoted as curve C, which conforms to the structural constraints of the surrogate model. The final shape of the complete surrogate model capability is a centrically symmetric hexagon, resulting from the combination of:

- The rectangular active/reactive power flexibility of the lumped storage and generator (Figure 11b, curve E),
- And the straight-line segment representing load curtailment capability (Figure 11b, curve F).

This hexagon is obtained by performing a rigid translation of the storage + generator rectangle along the direction defined by the load curtailment trajectory, which corresponds to increasing active power exchange from the distribution to the transmission system, with a slope determined by the selected power factor angle φ_L. To determine the reference power of the equivalent load, the following procedure is applied:

1. The rectangular capability of the combined lumped storage and generator is plotted in its original position, centered around the baseline operating point $P_0 - Q_0$.
2. This rectangle (curve E) is then translated along with the load reduction trajectory, simulating increasing demand curtailment.
3. The translation continues until one edge of the rectangle touches the numerically calculated capability boundary (curve B). At this point, the active power shift ΔP is measured (Figure 11b), which defines the reference power of the surrogate load.

This geometric approach ensures that the surrogate model remains consistent with the actual flexibility limits of the distribution network, while preserving a compact and interpretable representation.

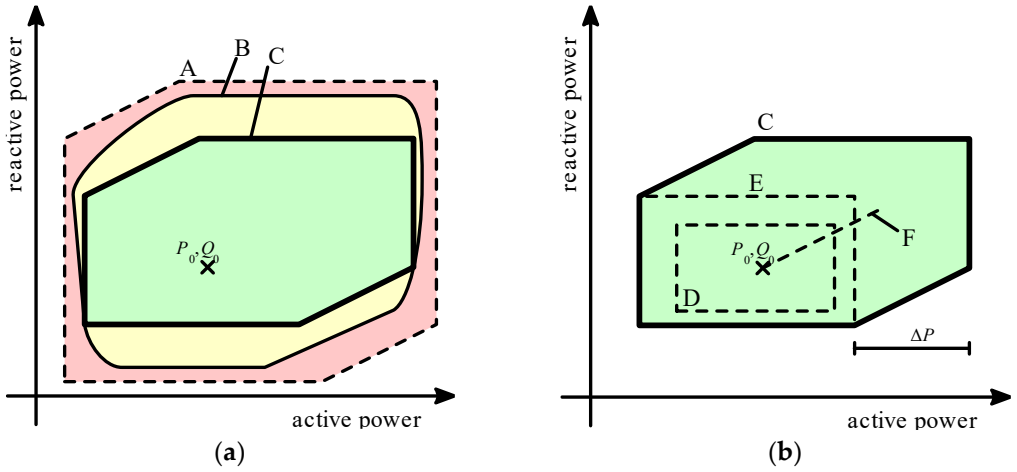


Figure 11. Equivalent capability of aggregated storage, generation, and load flexibility. P_0 and Q_0 (black cross) correspond to the active and reactive power exchange between distribution and transmission system. In (**a**) Curve A illustrates the aggregated flexibility of all storage, generation and load units without considering grid constraints. Curve B shows the aggregated flexibility after accounting for grid constraints. Curve C represents the combined capability curve of the surrogate storage, generation and load elements. (**b**) reports the details of Curve C, where Curve D indicates the portion of the total capability attributable to the surrogate storage, curve E the one attributable to surrogate storage and generation, F the one attributable to the surrogate load.

Thanks to the geometrical method described previously, the baseline active power consumption of the lumped load can be directly extracted:

$$P_L^{base}(t) = \Delta P(t) \tag{12}$$

This value represents the reference point around which the load flexibility is modeled and plays a key role in defining the surrogate model behavior. However, as shown in Figure 12, the resulting profile does not perfectly match the actual reference consumption observed across the full distribution network. This deviation is a natural consequence of the simplifications introduced by the surrogate model. Since it cannot represent all possible operating points (especially under complex network conditions) it tends to underestimate the load curtailment potential, particularly in situations where flexibility is constrained by topology or dispatch priorities.

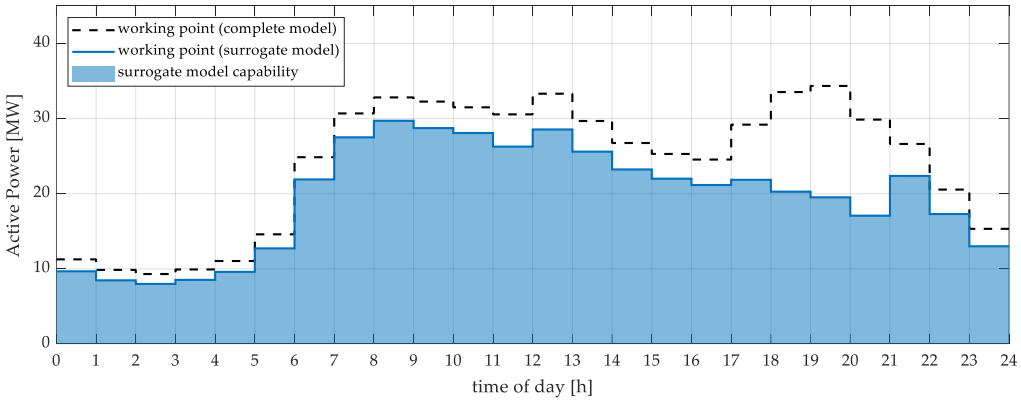


Figure 12. Time evolution of the baseline active power of the surrogate load, compared with the total consumption profile of the complete distribution network model.

At this stage, and recalling Section 2.3, the surrogate model now includes all necessary parameters for its three core elements (storage, generator, and load) except for the baseline

active and reactive powers of the lumped generator. These quantities are essential to ensure that the surrogate model remains centered around the actual power exchange profile between the transmission and distribution networks, which are obtained from the full network model (Section 2.1—Figure 4). Since the reference power profile of the lumped load is already known, the condition required to maintain this alignment can be imposed through:

$$\begin{cases} P_G^{base}(t) = P_0(t) - P_L^{base}(t) & \text{active power baseline of generation} \\ Q_G^{base}(t) = Q_0(t) - P_L^{base}(t)\tan(\varphi_L) & \text{reactive power baseline of generation} \end{cases} \quad (13)$$

3. Analysis of the Obtained Surrogate Model

Thanks to the procedure described in Section 2, the entire distribution network can be effectively approximated using a surrogate model composed of a limited number of lumped components (a storage unit, a generator, and a load). The parameters of these elements are optimally tuned to maximize the correspondence between the surrogate model's capability and that of the complete network.

The model extraction relies on a computationally efficient iterative process, based on low-demand algorithms, including the numerical reconstruction of flexibility capabilities [24]. This makes the proposed method particularly suitable for evaluating a large number of operating conditions, such as time series analyses or stochastic simulations, and benefits from being built upon conventional OPF algorithms. Naturally, the process introduces approximations, and as shown in Figure 13, the matching between the surrogate and complete models is not perfect and varies depending on the operating conditions of the distribution network. The degree of matching is assessed by comparing the areas of the actual (curve B in Figure 11a) and surrogate capabilities (curve C in Figure 11a). The results show that:

- The best correspondence occurs during the morning hours (5:00 ÷ 12:00), when load demand is high and helps counterbalance local generation, reducing congestion. In these conditions, the surrogate model achieves a maximum matching of 84%.
- The worst correspondence is observed during the evening and early morning (18:00 ÷ 5:00), when demand is low and high generation leads to network saturation. In these cases, flexibility margins are reduced, and the surrogate model matches the complete one by only about 60%.

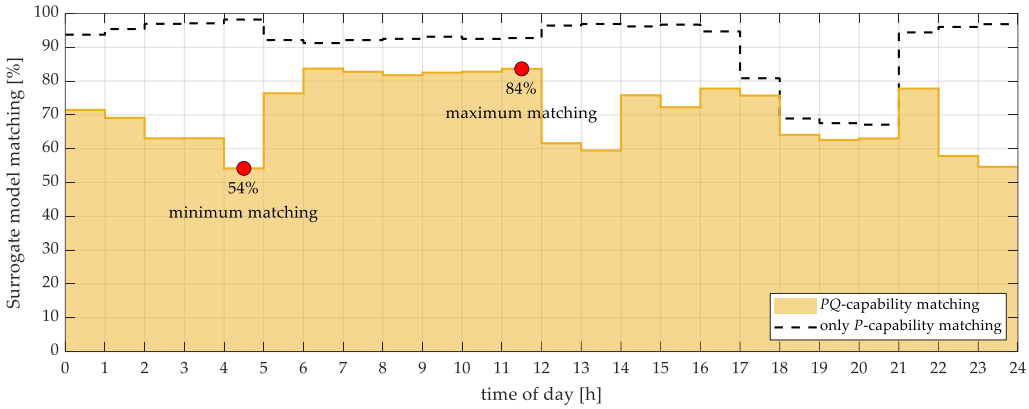


Figure 13. Matching between the power capability of the actual distribution network and its surrogate model. The yellow area illustrates the ratio between the *PQ*-capability region of the surrogate model and that of the complete distribution network. The dashed black line compares the active power flexibility margins of the two models.

Since the surrogate model is primarily designed to support flexibility services based on active power, it is also meaningful to assess its performance in representing reactive power flexibility. Interestingly, results show that the active power matching is significantly better than that of the full capability curve, with values exceeding 90% for most of the time. Notable discrepancies occur during evening hours, when peak loads and the heterogeneity of load power factors reduce the accuracy of the model.

By analyzing the time periods with the best (Figure 14a) and worst performance (Figure 14b), it becomes clear that the complete and surrogate models yield different flexibility capabilities. However, as shown in Figure 14, the capability of each individual component within the surrogate model consistently overlaps with the corresponding numerically calculated capability from the complete model, even in the worst case.

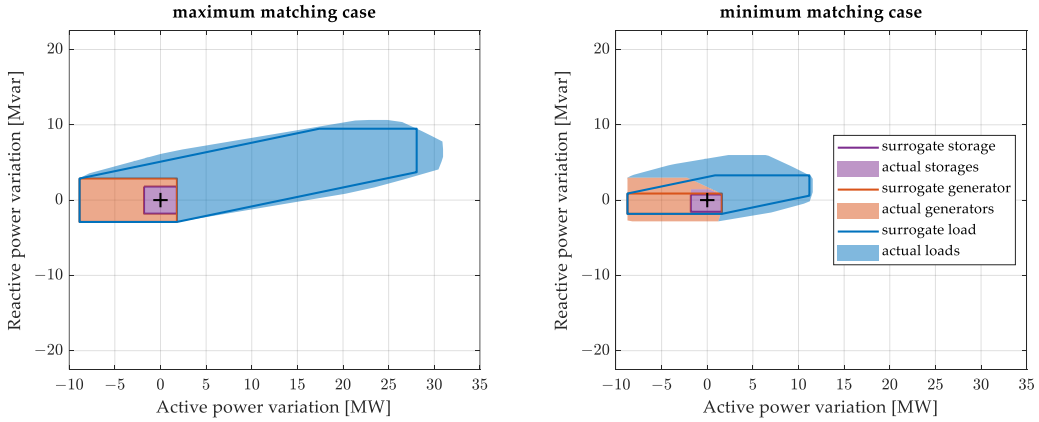


Figure 14. Capabilities computed for the complete distribution network and for the surrogate model: (**a**) shows the case with the highest matching between the two models; (**b**) illustrates the case with the lowest matching, highlighting the impact of network constraints and surrogate model simplifications. Crosses indicate the origin of the active–reactive power variation plane, corresponding to operating points where no flexibility exchange occurs between the distribution and transmission networks. These points represent the absence of flexibility services being provided by the distribution system.

According to this analysis, the surrogate model presents both strengths and limitations that must be carefully considered. First, the overall matching with the full PQ-capability curve of the distribution network is not particularly high, especially when considering the entire active–reactive power domain. This is partly due to the fact that the model was not designed to maximize the matching performance, but rather to prioritize the delivery of active power flexibility, where matching results are significantly better.

Importantly, the surrogate model returns a capability that is a subset of the actual distribution network flexibility, ensuring that any request formulated by the TSO is always implementable in practice, albeit not necessarily optimal. In this sense, optimality is not a core objective of the model; instead, the focus is placed on implementability, simplicity of communication between DSO and TSO, and robustness.

Moreover, the matching performance can be improved by increasing the number of surrogate elements used in the model (from the current three to a larger number N) thus enhancing the representativeness of the distribution network. Looking ahead, the construction procedure could be extended to automatically determine the optimal number of surrogate elements required for a given network, introducing refinements and automation in Step 2 of the computation procedure (Figure 3).

4. Application of the Surrogate Models for Distribution Flexibility Integration in Transmission Resilience Enhancement Framework

This section describes the application of surrogate models to exchange data between TSOs and DSOs, with the final aim of modeling the flexibility of distribution network to support transmission system resilience. Indeed, flexibility connected to the distribution network allows for the management of local congestion and control over the exchange profile with the transmission network simultaneously. The latter function can provide crucial support for managing contingency situations at the transmission network level, which might require, for example:

- Limiting the exchange of active/reactive power in the primary substation.
- Increasing the counter-flow of energy to supply a portion of the load belonging to neighboring distribution networks.
- Participating in voltage regulation by modulating the reactive power exchanged between the transmission and distribution systems.

In these circumstances, the DSO can act as a technical aggregator of the flexible resources belonging to the distribution networks involved and communicate their actual availability in real-time in an aggregated manner. In this way, each individual distribution network is seen by the TSO as a set of three (or more) independent sources of flexibility (storage, generator and load) according to the following procedure:

- The DSO collects information on the operating status of the individual resources and estimates their potential in terms of varying the power flow in the primary substation (while considering the constraints of the distribution network).
- The DSO communicates the overall flexibility potential to the TSO, in terms of possible changes in active and reactive power.
- The TSO evaluates the conditions of its own network and, based on the actual flexibility available, communicates the optimal set-point to the DSO.
- The DSO receives the information, disaggregates it, and communicates the optimal set-points to the flexible resources involved.

Thus, in the context of a possible coordinated framework between TSOs and DSOs for transmission resilience enhancement, surrogate models provide a simple representation of the potential flexibility of distribution networks, preserving the confidentiality of data among different operators, and exchanging the minimum amount of data needed to define specific services supporting transmission system resilience.

4.1. Coordinated Framework for Resilience Enhancement

This application analyses the main features of the coordinated framework for resilience enhancement on transmission network, including the integration of the distribution network surrogate model. The coordinated framework aims at minimizing the power system degradation, i.e., the impacts due to the foreseen extreme events, by identifying cost-effective preventive and corrective actions in the short term (e.g., next 15 min or 1 h). It analyses a set of contingencies (obtained by combining threats and asset vulnerabilities), considering system recovery process, as well as several sources of uncertainties such as component vulnerability to the threats. System degradation is quantified by a metric related to power supply performances, as explained below. Given the short-term operational context, uncertainties about threat forecasts and load demand and renewable generation can be considered negligible.

In line with the methods mentioned in [27], the framework relies on an optimization that pursues the best trade-off between the degradation metric and the cost of the (preventive and corrective) measures implemented to face the multiple contingencies. Incidentally,

the framework limits the probability of inception of cascading outage phenomena. The set of multiple contingencies is characterized in probabilistic terms, by accounting for the grid asset vulnerabilities and the threat features (severity, location, etc.) in the next time interval of analysis. The currently adopted degradation metrics is the Conditional Value At Risk (CVAR) of the distribution of a suitable impact metrics [28].

The impact metric adopted in the proposed framework formulation is the Cost of the Energy Not Served (CENS) to the customers, because this metric is of great interest for regulatory authorities. This metric also accounts for the restoration process. In fact, the recovery phase of faulty components represents an important aspect in resilience analyses: a delay in the repair of the infrastructure can lead to delays in the reactivation of the electricity service and therefore higher values of energy not supplied. For this reason, the framework proposed in [29] includes a recovery model of failed components.

Several active measures are used to minimize system performance degradation. The modeling of the power capability of the surrogate model components (storage, generator and load) presented in Sections 2 and 3 is carried out considering that the distribution network can provide services in terms of both preventive actions and corrective actions, which are appropriately valued in terms of costs:

- Preventive actions consisting of:
    - Modification of the set-point of the generation component of the surrogate model within the capability.
- Corrective actions consisting of the following actions on the surrogate model:
    - Modification of the power set-point of the generation component.
    - Reduction in the power absorbed by the load component.
    - Absorption and/or injection of power by the storage.

For comparison purposes, also an uncoordinated framework condition is also represented, for which only corrective actions are applied consisting of load shedding and disconnection of the surrogate network generation (typical actions performed in an emergency by network operators).

It is worth highlighting that only the active power capability of the surrogate model of distribution system for the provision of services to the transmission network is integrated into the coordinated framework, since the coordinated framework is based on a DC load flow formulation.

4.2. Application Results

The application case study consists in an integrated high- and medium-voltage system where the transmission network is the IEEE 118 bus system [30] to which the surrogate model of the distribution network presented in Section 2 is connected (Figure 15). A simulation case is completely set when the following aspects are defined:

(1) The threat evolution (whereby components are struck by threat at specific hours of interest, thus, the most probable contingencies affecting the system can be identified).
(2) The operating point of the power system: in quasi-real-time operation the uncertainties concerning forecast errors on load demand and renewable generation can be considered negligible.
(3) The distribution network behavior in case of severe contingencies affecting the transmission system.
(4) The localization and configurations of distribution networks.
(5) The cost profile for the ancillary services from distributed resources to support transmission system resilience.

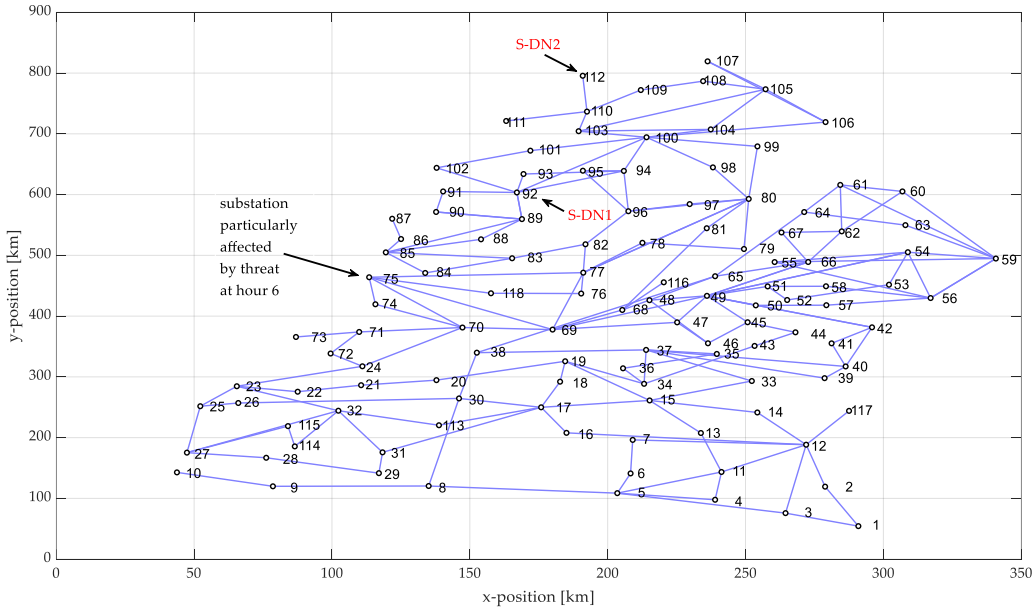


Figure 15. Georeferenced one-line diagram for the power system under test (IEEE 118-bus system), with indications on the position of the considered distribution networks (bus 92 and bus 112) and with focus on the hour 6 of the threat evolution trajectory.

As far as point (1) is concerned, a simplified interaction power system-threat model is adopted to evaluate the set of most probable multiple contingencies affecting the power system at specific hours, starting from reasonable hypotheses about the threat evolution. Specifically, the simulation results are focused on hour 6 of the threat evolution over time. In this hour, 32 contingencies are foreseen with their probabilities of occurrence (which are derived in turn from the failure probabilities of the components affected by threat at hour 6). In particular, five branches connected to bus 75 (i.e., 70–75, 69–75, 74–75, 75–77, 75–118) are identified as "critical components", i.e., components with the highest failure probabilities. From these components, a set of 32 contingencies (including "null" contingency) is derived considering all the combinations of k outaged components over the set of the abovementioned components (thus, five N-1, five N-4 outages, ten N-2, ten N-3 and one N-5 contingencies). Figure 16 indicates the outaged components (in blue) for each contingency ID considered in the analysis.

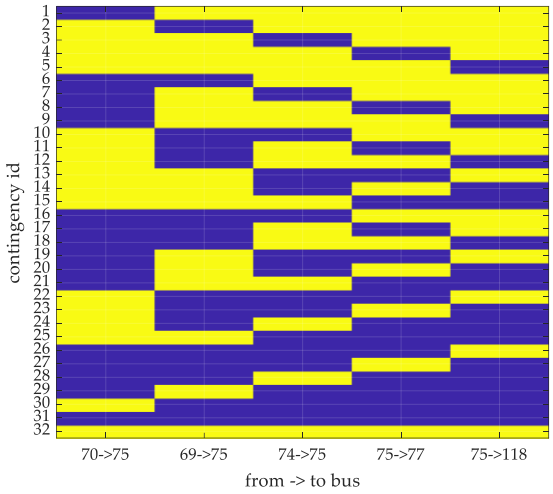


Figure 16. Indication of outaged components (in blue) and of components in service (in yellow) for each of the contingencies under analysis. CTG 32 represents the "null" contingency (i.e., no component outages).

Bus 75 is strongly affected by the threat and contingency 31 causes the loss of all the branches connected to bus 75. A five-hour recovery time is assumed for all the grid components in the present case study.

As far as point (2) is concerned, the same operating point for the IEEE 118 bus test system described in [31] is adopted.

With reference to point (3) above, three types for responses from distribution network resources in case of contingencies are considered:

- Operation 1: distribution resources provide ancillary services for resilience support to the transmission system
- Operation 2: distribution resources intervene in case of emergencies by shedding at high costs a fraction of the total load and/or generation components.
- Operation 3: distribution resources do not intervene in case of contingencies: in case of nodal power imbalance at their point of common coupling due to the loss of connectivity to the transmission system, they open the breaker of primary substation and start working with zero power exchange (islanded mode).

As far as point (4) is concerned, a former distribution network (henceforth named "S-DN 1") presented in Section 2 is assumed to be connected to bus 92, which is represented by means of its surrogate model (discussed in Section 3). To further study the contribution of distribution resources to the proposed case study, an identical distribution network (henceforth named "S-DN 2") is also assumed to be connected to bus 112.

Three cost profiles are assumed for the provision of resilience support ancillary services from the considered distribution resources:

- Profile A: medium costs for upward and downward variations of the distribution network power exchanges.
- Profile B: high costs for upward and downward variations of the distribution network power exchanges.
- Profile C: low costs for upward and downward variations of the distribution network power exchanges.

Table 1 compares the specific costs for the surrogate model of distribution network for the three profiles. Instead, as far as the transmission system based resources are concerned, the unitary costs of preventive upward and downward redispatch for conventional generators are set to 100 and −20 amu/MWh, while the renewable corrective curtailment is 1000 amu/MWh, and the load shedding unitary cost is 40,000 amu/MWh. Table 2 lists the described simulations.

Table 1. Unitary cost parameters for the three cost profiles adopted for simulations.

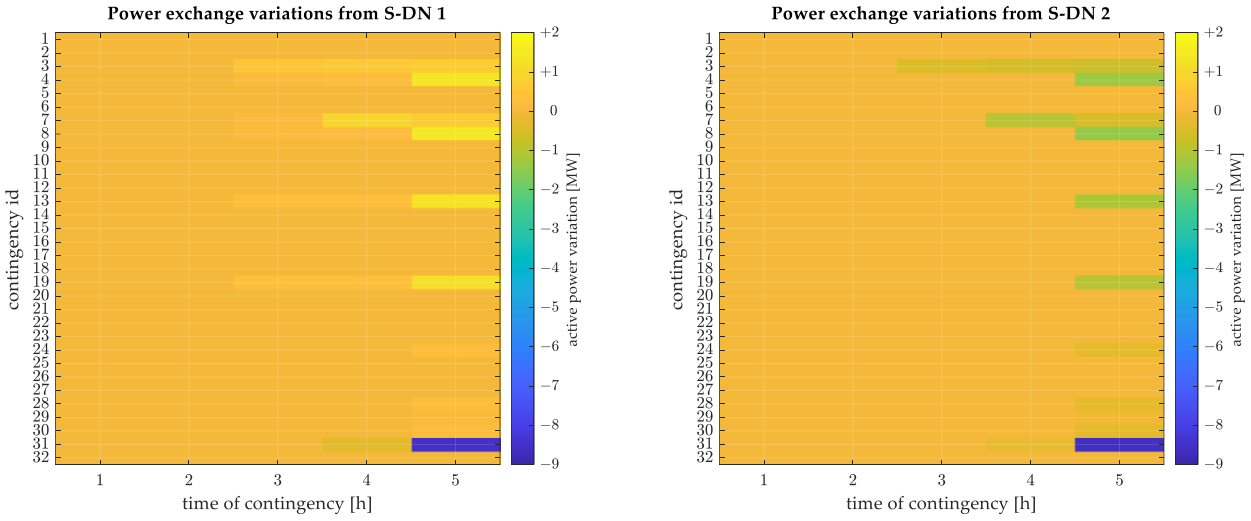
Quantity	Costs [amu/MWh]		
	Profile A	**Profile B**	**Profile C**
unitary cost for charge of surrogate storage	−20	−50	−5
unitary cost for discharge of surrogate storage	100	400	20
unitary cost for upward variation of surrogate generator	150	400	20
unitary cost for downward variation of surrogate generator	−20	−50	−5
unitary cost for curtailment of surrogate load	25,000	25,000	25,000
unitary cost for load shedding (no ancillary services)	40,000	40,000	40,000
unitary cost for generation shedding (no ancillary services)	500	500	500

Table 2. List of simulation cases.

Case ID	Operating Behavior	Cost Profile
A1	1	A
A2	2	-
A3	3	-
B1	1	B
C1	1	C

4.2.1. Provision of Ancillary Services at Moderate Costs (A1)

This case assumes that two identical surrogate models are connected to buses 92 and an to bus 112 of transmission grid. The two distribution networks provide ancillary services to support resilience at moderate unitary costs. Results show that some corrective actions involving the two surrogate models are suggested at hours 2 through 5 for several contingencies (see Figure 17a,b): especially in case of contingency 31 (loss of all the branches connected to bus 75) their downward contributions by 16 MW at hour 5 allows to reduce the amount of generation shed at that hour (see Figure 18b) with respect to the case in which distribution network does not exchange ancillary services (see Section 4.2.1). The corrective actions on distribution resources for other contingencies allow avoiding the preventive shift in power from unit 36 to 34 as well as the load shedding at bus 2 in case of contingency nr. 19 (both facts occur in case A3 with no contributions from distribution networks).



(**a**) (**b**)

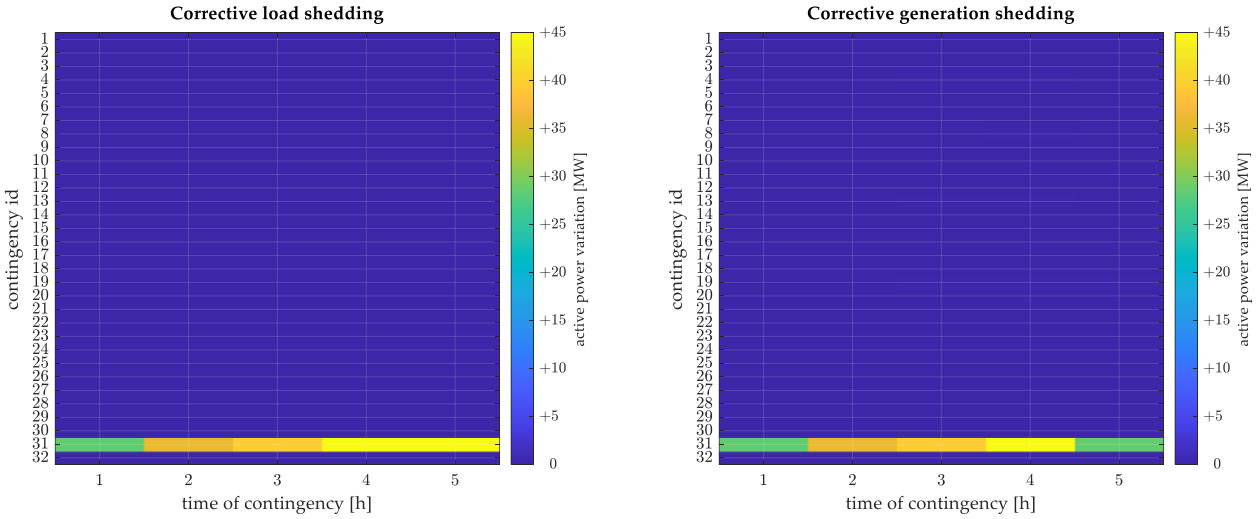
Figure 17. Corrective power exchange variations from (**a**) distribution network connected to bus 92 (S-DN 1) and (**b**) distribution network connected to bus 112 (S-DN 2) for the different contingencies at hour 6. Distribution resources providing ancillary services at moderate costs (case A1).

The CVAR is 0.4764 amu but the expected costs for corrective actions are 12.0178 amu, while no costs for preventive actions are required.

4.2.2. Load and Generation Shedding Automatisms (A2)

This simulation case considers the presence of shedding automatisms for the load and generation components of surrogate models: this means that, though distribution network resources do not provide ancillary services for resilience, in case of emergency (*N-k* contingencies) they can shed a fraction of the load and generation components of the surrogate capability curve, at higher costs with respect to the ones adopted in case of

provision of ancillary services: unlike case A1 (Section 4.2.1), the storage component is not used.



(**a**) (**b**)

Figure 18. Corrective (**a**) load shedding and (**b**) generation shedding actions at transmission level, while distribution network resources are providing ancillary services at moderate costs (case A1).

The analysis of Figure 19a,b shows that shedding automatism intervenes only at the distribution network connected to node 92 to several contingencies to relief potential overloads, thus avoiding the preventive shift in power from unit 36 to 34, as well as the load shedding at bus 2 for contingency 19 (both facts occurring in case A3—Section 4.2.3). No preventive actions are suggested. The final CVAR is 0.4764 amu; the expected costs for corrective actions (reported in Figure 20) are equal to 21.0837 amu (higher than in case A1 of ancillary services provision). It is worth noting that the adopted measure on distribution network resources do not contribute to reduce the generation shedding amount at contingency 31 in this case. It is worth noticing that the achieved CVAR is structurally limited by the most severe contingency (complete disconnection of node 75 due to an N-5 event) which cannot be mitigated by any control action. This explains why case A2 results in the same CVAR value as case A1, despite the different control strategies applied.

4.2.3. No Support from Distribution Resources, and Moderate Costs for Load Generation Shedding (A3)

In this case, the control suggests a preventive variation in the active power set-points for generating units 34 and 36, shifting about 0.3 MW from unit 34 to 36 (see Figure 21a,b), while in case of contingency 31 (loss of all branches connected to bus 75), the resilient control proposes a 45 MW peaking load shedding at bus 75 (Figure 22a) compensated by a corresponding generation shedding (in Figure 22b) equal to a maximum of 45 MW over 5 h at generators 31 through 42. Moreover, in case of contingency 19 the control suggests a small amount of load shed at bus 92 (0.032 MW, 0.016 MW and 0.041 MW for hours 3, 4 and 5). The availability of distribution network flexibility for resilience support allows to correctively adjust the operating point of the grid only in case of contingencies (see, for example, corrective power exchanges of the surrogate models in Figure 17 from case A1) in a economical way, avoiding the need for expensive preventive actions (which are performed independently from the actual occurrence of contingencies), as in the present case.

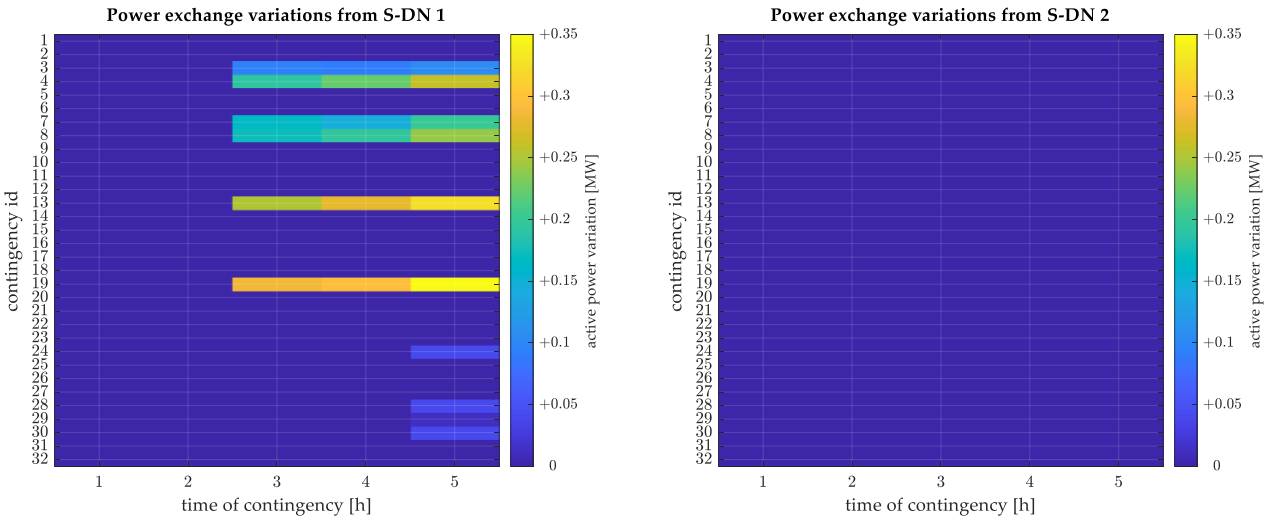


Figure 19. Corrective power exchange variations from (**a**) distribution network connected to bus 92 (S-DN 1) and (**b**) distribution network connected to bus 112 (S-DN 2) for the different contingencies at hour 6. Distribution networks equipped with automatic shedding schemes (case A2).

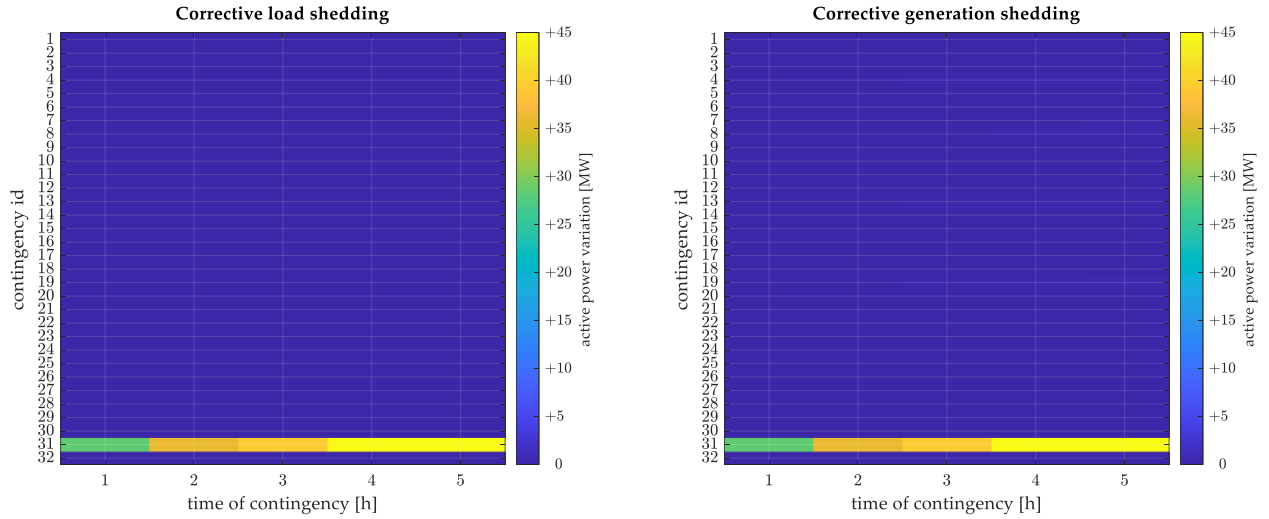


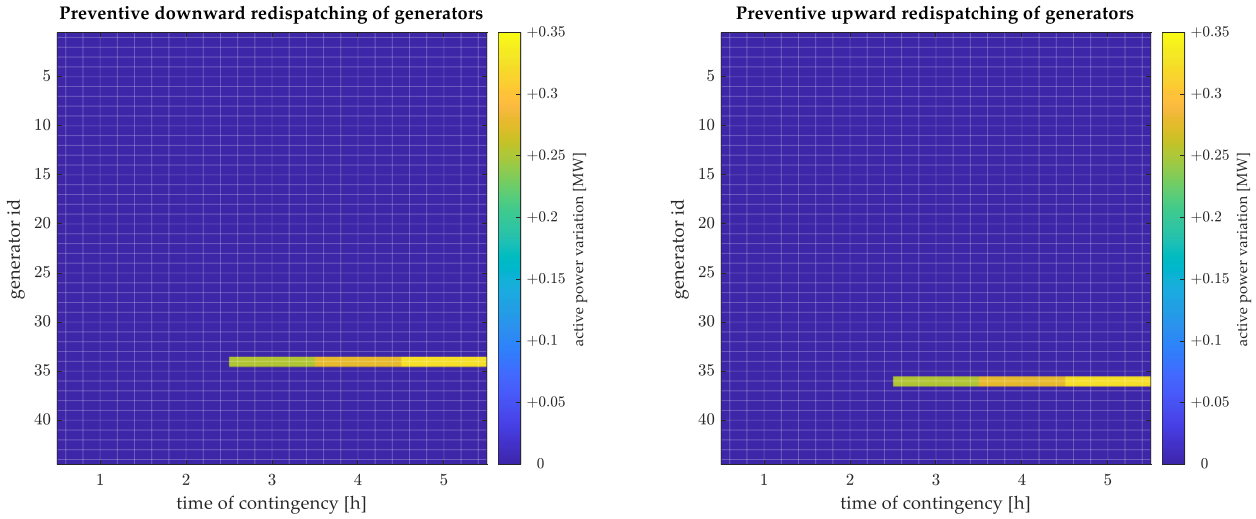
Figure 20. Corrective (**a**) load shedding and (**b**) generation shedding actions at transmission level., Distribution networks equipped with automatic shedding schemes (case A2).

The CVAR is equal to 0.8844 amu (higher than in previous cases), the expected costs for corrective actions are 0.0011 amu (much lower than in previous cases A1 and A2), but the actual costs for preventive actions are equal to 68.3990 amu (while no preventive actions are suggested in cases A1 and A2). No contributions come from distribution resources: the load and generation components of the surrogate models at buses 92 and 112 remain intact. Such simulation demonstrates that the absence of contribution from distribution means higher CVAR indicators with higher total costs for control actions.

4.2.4. Provision of Ancillary Services at High Costs (B1)

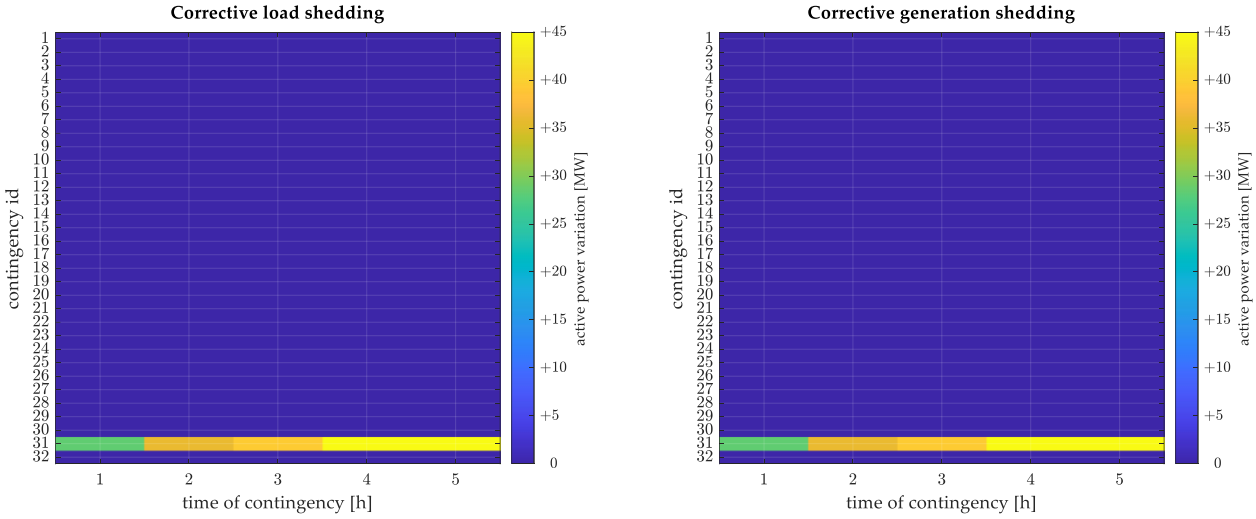
The pattern of load shedding actions suggested by this case is very similar to the one in Case A1: the CVAR is 0.4764 amu (the same as in Case A1) while the expected costs for corrective actions is equal to 18.975 amu (of course higher than 12 amu of case A1, due to the higher unitary costs for services provided by distribution resources). Another difference

consists in the fact that the control changes the distribution networks power exchanges by smaller amounts (see, for example in Figure 23a,b the total −12 MW variation is imposed to the two surrogate models for contingency 31, instead of −16 MW in previous case), given the higher costs for their deployment. This in turn implies higher generation shedding at hour 5 in case of contingency nr. 31 (32 MW against 28 MW of Case A1, as shown in Figure 24b) while load shedding remains the same of case A1 (Figure 24a).



(**a**) (**b**)

Figure 21. Preventive (**a**) downward and (**b**) upward redispacth actions on dispatchable generators. No support from distribution resources (case A3).



(**a**) (**b**)

Figure 22. Corrective (**a**) load and (**b**) generation shedding actions at transmission level. No support from distribution resources (case A3).

4.2.5. Provision of Ancillary Services at Low Costs (C1)

Also in this case, the control suggests the intervention of surrogate components to provide support to resilience of transmission systems (see Figure 25a,b). The pattern of load and generation shedding actions suggested by this case is again very similar to the one of Case A1 (see Figure 26): the CVAR is 0.4764 amu (same as Case A1) while the expected costs for corrective actions is equal to 4.8652 amu (of course lower than 12 amu of case A1, due to the lower costs for ancillary service provision). Another difference consists in the fact that

corrective actions on distribution resources are required over more hours (starting from hour 2 after contingency applications), thanks to the lower costs for their deployment. The intervention of distribution resources reduces the need for corrective generation shedding at hour 5 with respect to case B1, as shown in Figure 26.

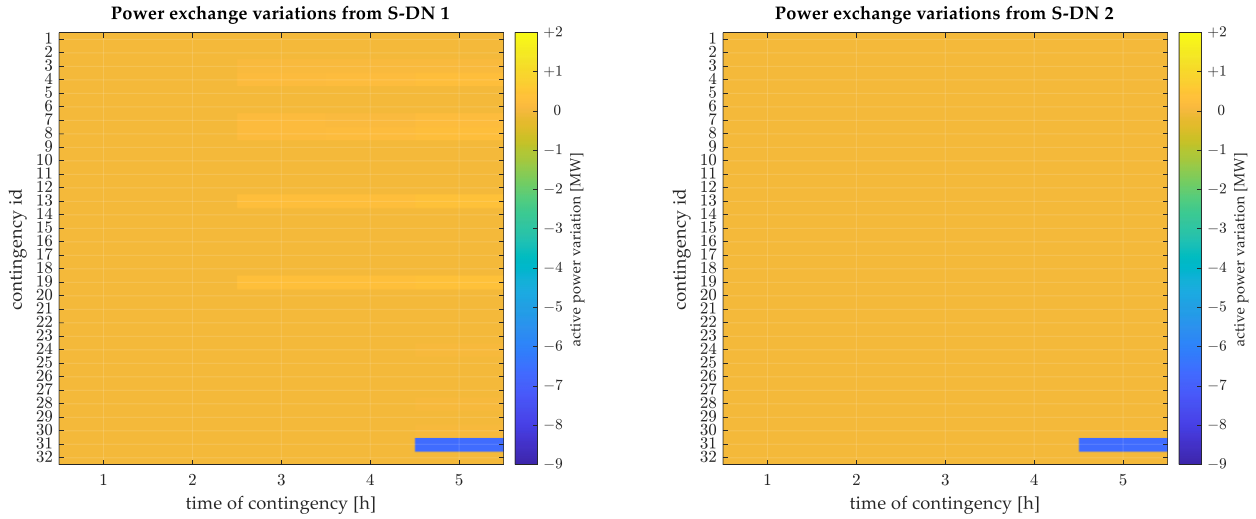


Figure 23. Corrective power exchange variations from (**a**) distribution network connected to bus 92 (S-DN 1) and (**b**) distribution network connected to bus 112 (S-DN 2) for the different contingencies at hour 6. Distribution resources providing ancillary services at high costs (case B1).

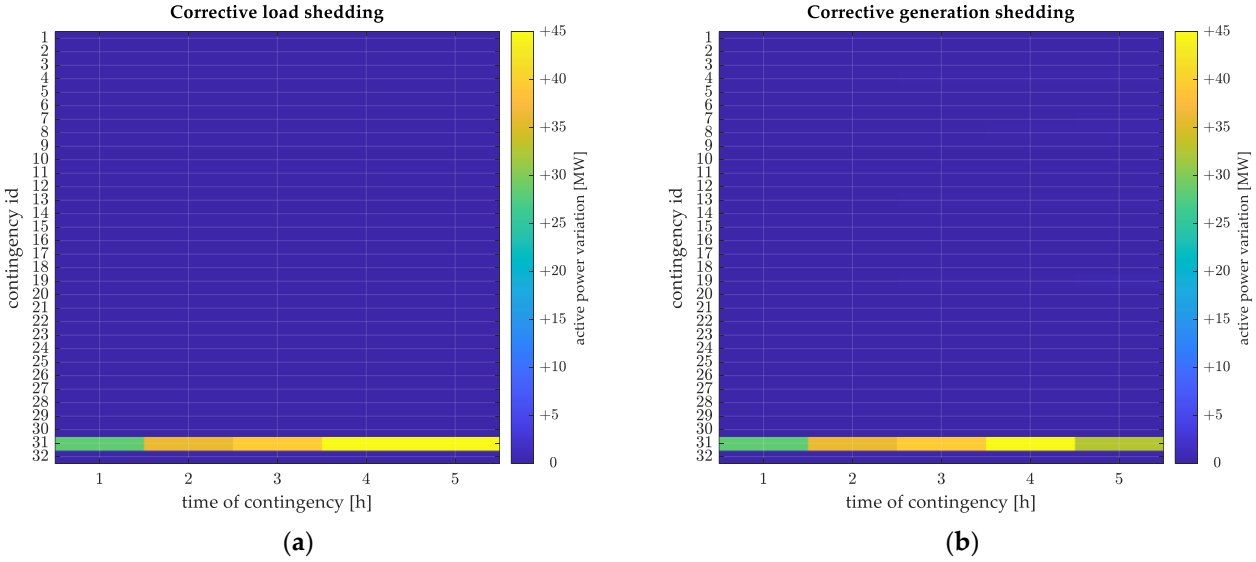


Figure 24. Corrective (**a**) load shedding and (**b**) generation shedding actions at transmission level, while distribution network resources are providing ancillary services at high costs (case B1).

4.3. Discussion of Surrogate Model Application and Disaggregation of Set-Points

The comparison of the simulation cases performed on the coordinated transmission and distribution case study allows to draw some final remarks:

(1) Surrogate models are very effective and easy to use for the integration of distribution network flexibility curves (and the relevant ancillary services) inside frameworks for TSO-DSO coordinated actions to support system resilience.

(2) The contribution from the ancillary services from distribution resources for resilience support allows to achieve lower costs for control actions (as highlighted by the

comparison between case A1 and cases A2, A3), possibly also attaining lower CVAR values (see cases A1 vs. A3).

(3) Simpler forms of interactions between distribution network and transmission system, such as emergency shedding schemes for load and generation (operation mode 2 in Section 4.2), can be useful to achieve the same minimum CVAR value as in case of ancillary services provision, but at higher expected costs for corrective actions (see cases A1 and A2).

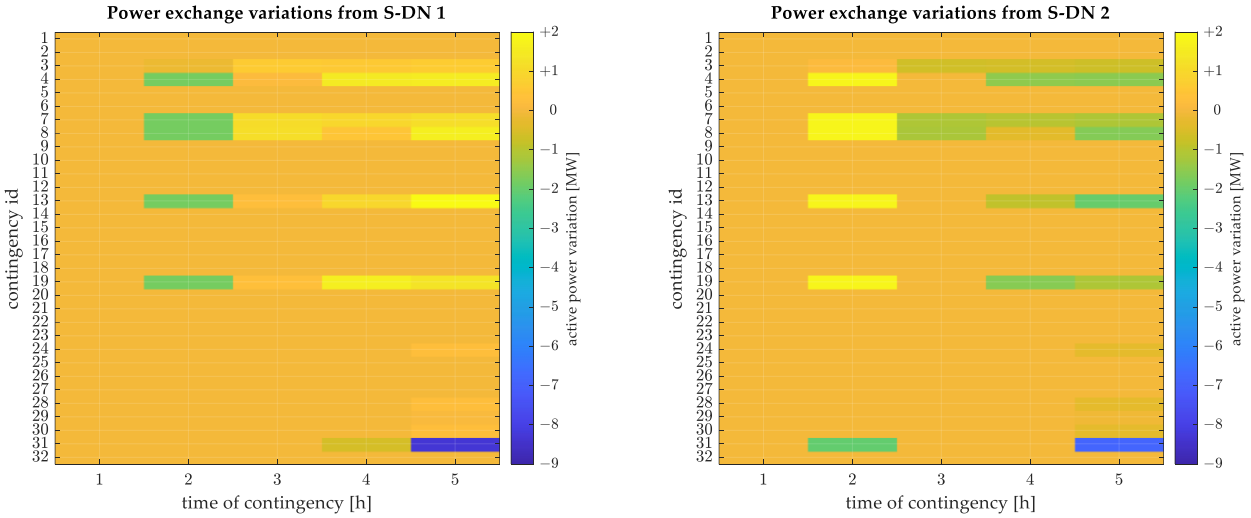


Figure 25. Corrective power exchange variations from (**a**) distribution network connected to bus 92 (S-DN 1) and (**b**) distribution network connected to bus 112 (S-DN 2) for the different contingencies at hour 6. Distribution resources providing ancillary services at low costs (case C1).

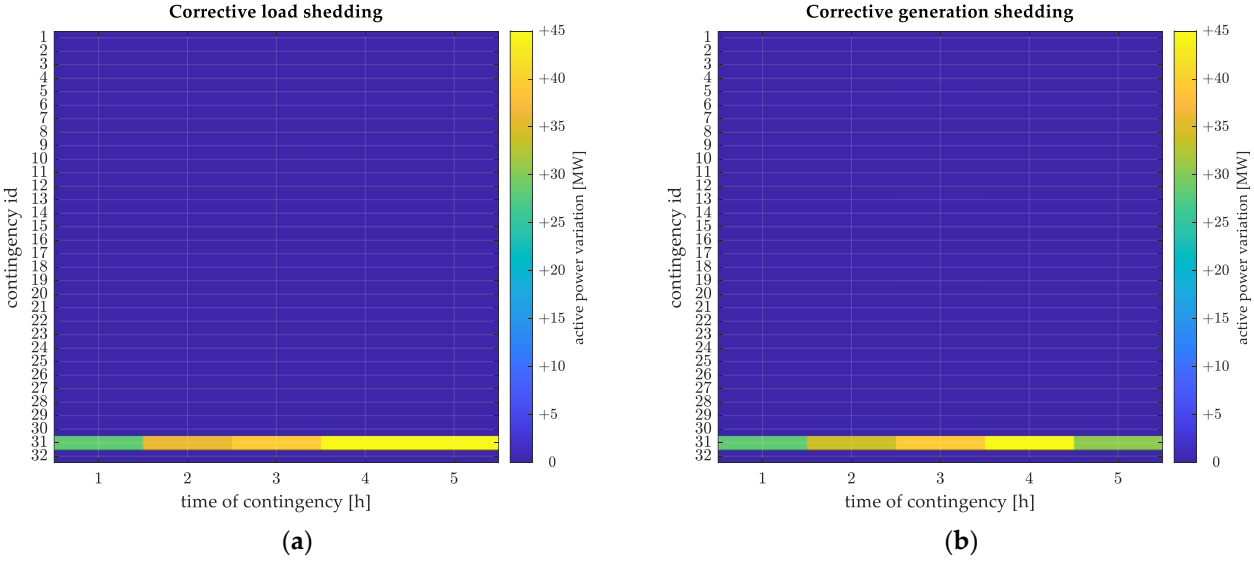


Figure 26. Corrective (**a**) load shedding and (**b**) generation shedding actions at transmission level, while distribution network resources are providing ancillary services at low costs (case C1).

From the results reported in Section 4.2, it can be noticed how the price of ancillary services from distribution resources directly influences the requested volume of flexibility. As expected, lower prices lead to higher volumes of contribution from distributed resources, which are aggregated through the surrogate model. This behavior confirms the economic

sensitivity of flexibility activation and highlights the importance of pricing mechanisms in shaping resource participation.

The following subsections explore how different set-points assigned to the surrogate model affect the activation of distribution resources, i.e., the disaggregation process that translates system-level commands into local dispatching actions. As an illustrative example, the analysis focuses on contingency case 31, applied to the distribution network represented by surrogate model S-DN1. This situation is considered one of the most critical, and therefore particularly relevant for evaluating the performance of the surrogate model under stress conditions.

This analysis focuses on cases where the surrogate model plays an active role in coordinating flexibility (A1, B1, C1) and therefore excludes A2 and A3. These two cases are not particularly relevant from the perspective of surrogate modeling: A2 involves conventional load and generation automatic shedding schemes within the distribution network, while A3 refers to islanded operation of the distribution system. In both situations, the surrogate model serves only as a source of information for the TSO, indicating either the volume of load and generation available for curtailment or the feasibility of fully disconnecting the distribution network from the transmission grid. Consequently, the DSO does not need to perform any post-processing of the surrogate model's set-points but simply acts by shedding load and/or generation or isolating the network.

4.3.1. Variation in the Active Power Exchange at the TSO-DSO Interface

The resulting active power variations, shown in Figures 17a, 23a and 25a, are plotted relative to the total active power exchange of SDN-1 (Figure 27). During the 5 h contingency period, the profiles of cases A1, B1, and C1 clearly deviate from the baseline, in which no ancillary services are requested by the TSO from the DSO. A more detailed analysis reveals an additional deviation in the time window between 14:00 and 17:00, which is attributed to the behavior of storage units. These units, having been activated during the contingency to support system resilience, subsequently restore their internal energy, thereby affecting the overall power exchange profile.

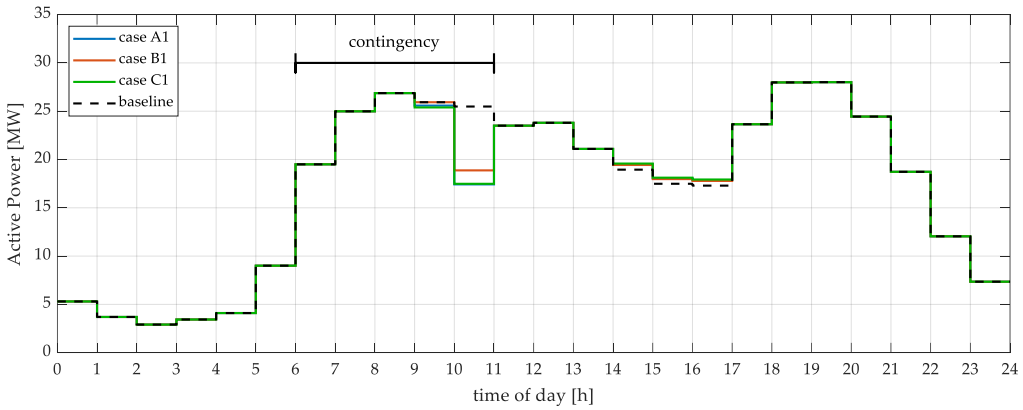


Figure 27. Total active power exchange from transmission to distribution system in cases A1, B1, and C1. Contingency 31 is used to analyze the behavior of the distribution network modeled by S-DN1.

These results are the outcome of a disaggregation process, which can be implemented in various ways. Referring to Figure 1, disaggregation occurs immediately before dispatching orders are sent: the DSO can either re-optimize the distribution network to jointly address local operational needs and the power variation requested by the TSO, or alternatively, disaggregate the surrogate model set-point into individual resource set-points that do not interfere with local congestion management actions. Both approaches are feasible, but they involve fundamentally different disaggregation procedures.

In the current example, disaggregation is performed by running an optimization that enforces the power deviation requested by the TSO during the contingency hours. Crucially, the surrogate model guarantees the feasibility of this OPF process, as it is constructed to ensure that any set-point communicated to the TSO corresponds to a physically implementable configuration within the distribution network.

4.3.2. Active Power Set-Points for Individual Storage Units

By imposing the active power variation at the TSO-DSO interface, the optimization adjusts the set-points of the storage units according to their available power capacity (Figure 28). In all considered cases, the storage units alone are insufficient to fully meet the active power variation requested by the TSO, particularly during hour 5 of the contingency (10:00–11:00), where the returned set-points saturate against the capabilities of the three units.

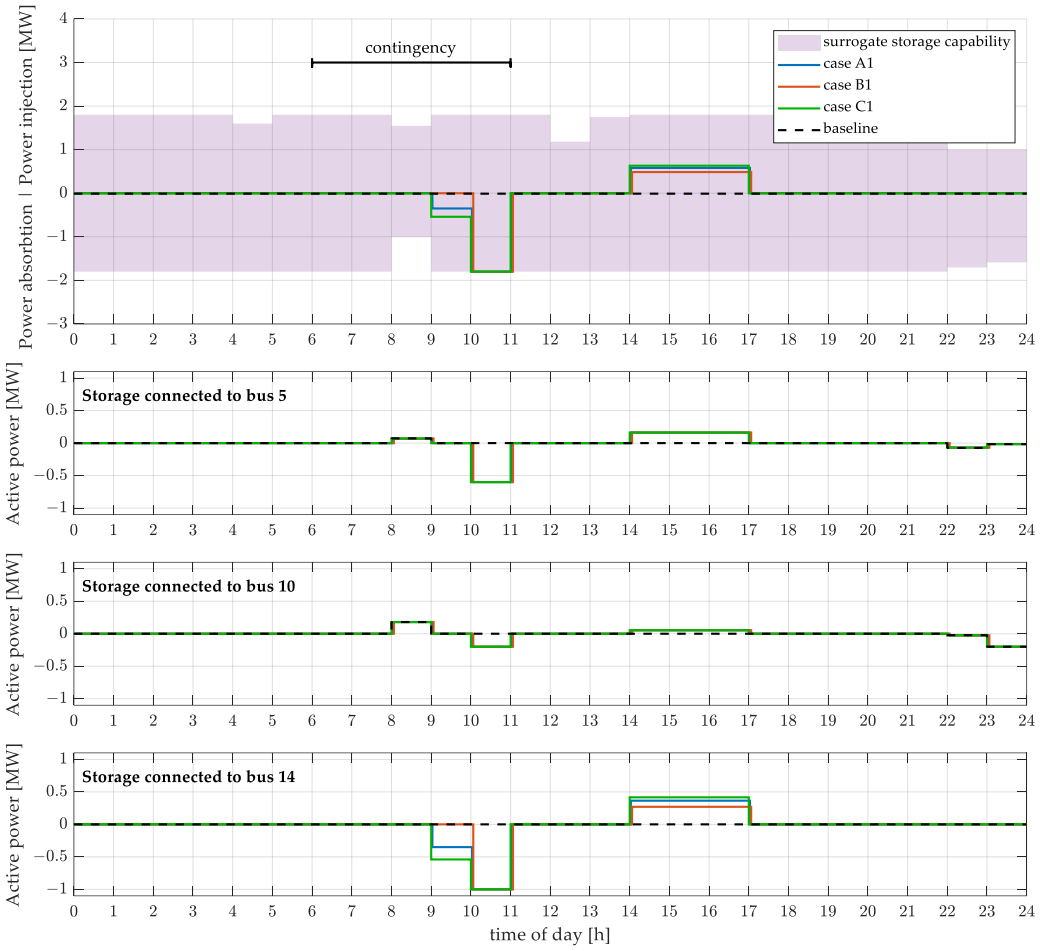


Figure 28. Total and individual active power exchange of storage units in cases A1, B1, and C1. Contingency 31 is used to analyze the behavior of the distribution network modeled by S-DN1.

Interestingly, power variations occurring at 8:00, 22:00, and 23:00, which are determined by the optimization for local congestion management (see Figure 5), are preserved, even though they are not explicitly represented in the surrogate storage model. This confirms that the surrogate model, while abstracted, does not interfere with local operational priorities.

Furthermore, the optimization of storage units has been carried out with the constraint of restoring the state of charge to its initial value by the end of the day. For this reason, after the contingency period, the constraints on TSO-DSO power exchange are relaxed to allow

the storage units to inject the energy accumulated during the contingency hours (see the time slot 14:00–17:00).

4.3.3. Active Power Set-Points for Individual Generation Units

The second element in the selected merit-order list is represented by the generation units, whose behavior in the simulated cases is shown in Figure 29. Among them, the large wind generator connected to bus 7 emerges as the main contributor to active power flexibility, with curtailment exceeding 5 MW during the contingency hours. This shedding occurs only when the storage units are no longer able to provide additional flexibility, specifically during contingency hour 5 (10:00–11:00). The remaining generators are collectively an order of magnitude smaller and contribute only to cases A1 and C1, while case B1 relies exclusively on the availability of the wind generator.

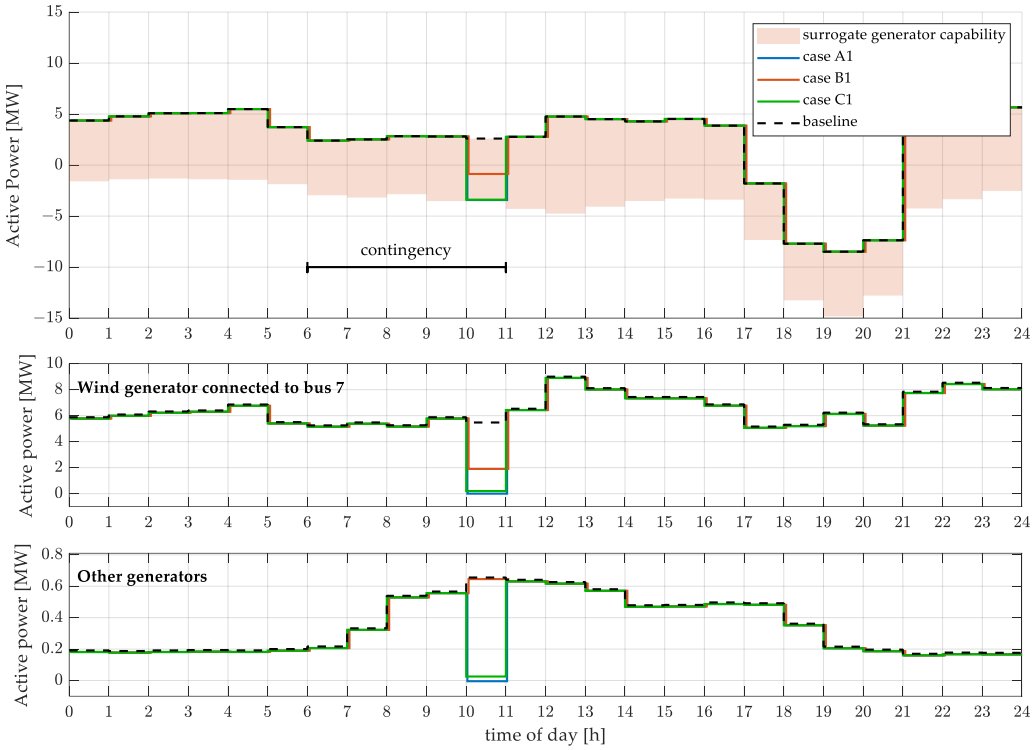


Figure 29. Total and individual active power exchange of generation units in cases A1, B1, and C1. Contingency 31 is used to analyze the behavior of the distribution network modeled by S-DN1.

4.3.4. Application of Reactive Power Set-Points

Reactive power set-points are typically processed by TSOs through separate procedures, mainly aimed at voltage regulation and power factor compensation in transmission networks [19]. For this reason, in this study, the contribution of reactive power from the distribution network (via the surrogate model) is analyzed independently from the active power variations.

Specifically, at hour 14:00, when the contingency is resolved and storage units are restoring their state of charge (causing a variation in active power exchange), three different reactive power requests from the TSO are simulated (see Figure 30):

- Case α: The reactive power variation is fully satisfied by the storage units.
- Case β: The reactive power variation requires additional support from generation units to meet the TSO request.
- Case γ: Although the reactive power variation could theoretically be satisfied using only storage and generation units, the approximation introduced by the surrogate

model leads to load curtailment to fulfill the request (resulting in a suboptimal disaggregation of set-points).

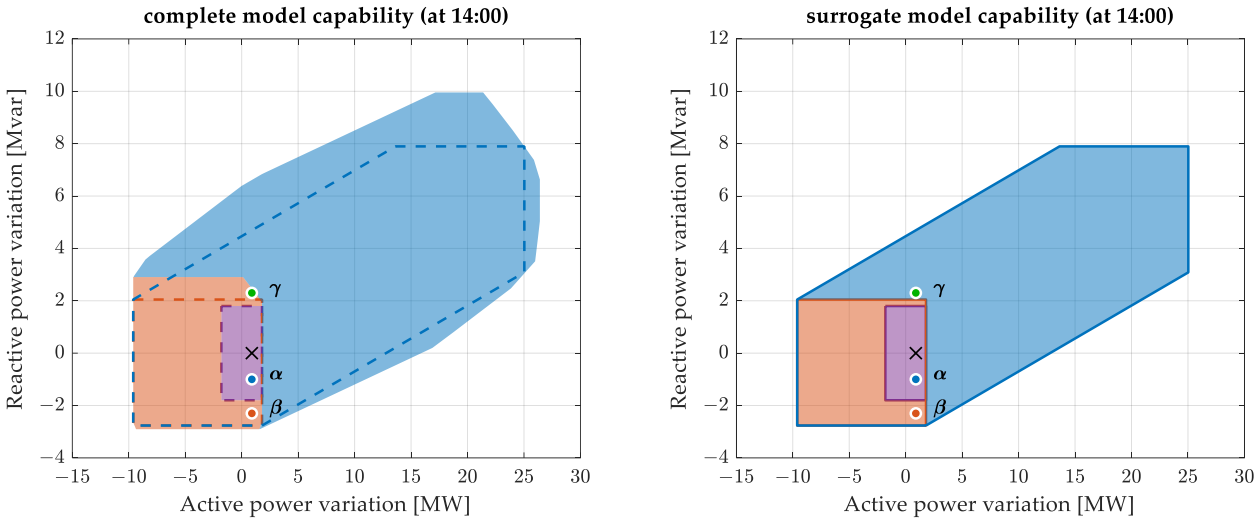


Figure 30. Capabilities of the complete distribution network (**a**) and surrogate model (**b**). Crosses indicate the original operating point before the reactive power variation. Round markers represent three simulated set-points requested by the TSO. The purple region denotes the storage capability, the orange region the generator capability, and the blue region the load capability, each shown as (**a**) actual and (**b**) surrogate. In (**a**), dashed lines indicate the boundaries of the surrogate model, included to facilitate comparison with the complete model.

As shown in Figure 30, case γ is particularly relevant for evaluating the surrogate model performance. Figure 30a demonstrates that the requested reactive power point lies within the theoretical operating region of the generators (orange area), while Figure 30b shows that the surrogate model fails to exploit this possibility and instead resorts to load curtailment (blue area) to meet the reactive power demand. Moreover, due to the load model adopted (see Section 2.4), reactive power variation also implies active power shedding, further impacting the distribution network.

Similarly to active power variation, reactive power is processed through an OPF by imposing, for the considered time step, both the current value of active power exchange and the requested reactive power exchange at the TSO-DSO interface. The resulting reactive power set-points for each distribution resource are shown in Figure 31, where the following behaviors can be observed:

- Storage units participate in all cases, being the first elements in the merit-order list. In particular, case α is characterized by the activation of the storage unit connected to bus 14 only, as its contribution is sufficient to meet the reactive power request.
- Generation units are involved in cases β and γ, supporting the storage units. In case γ, their contribution is limited by grid constraints (see Figure 30a).
- Loads are required to reduce their active power consumption by more than 1 MW to adjust the total reactive power and provide the remaining 0.26 MVAr that cannot be delivered by other resources.

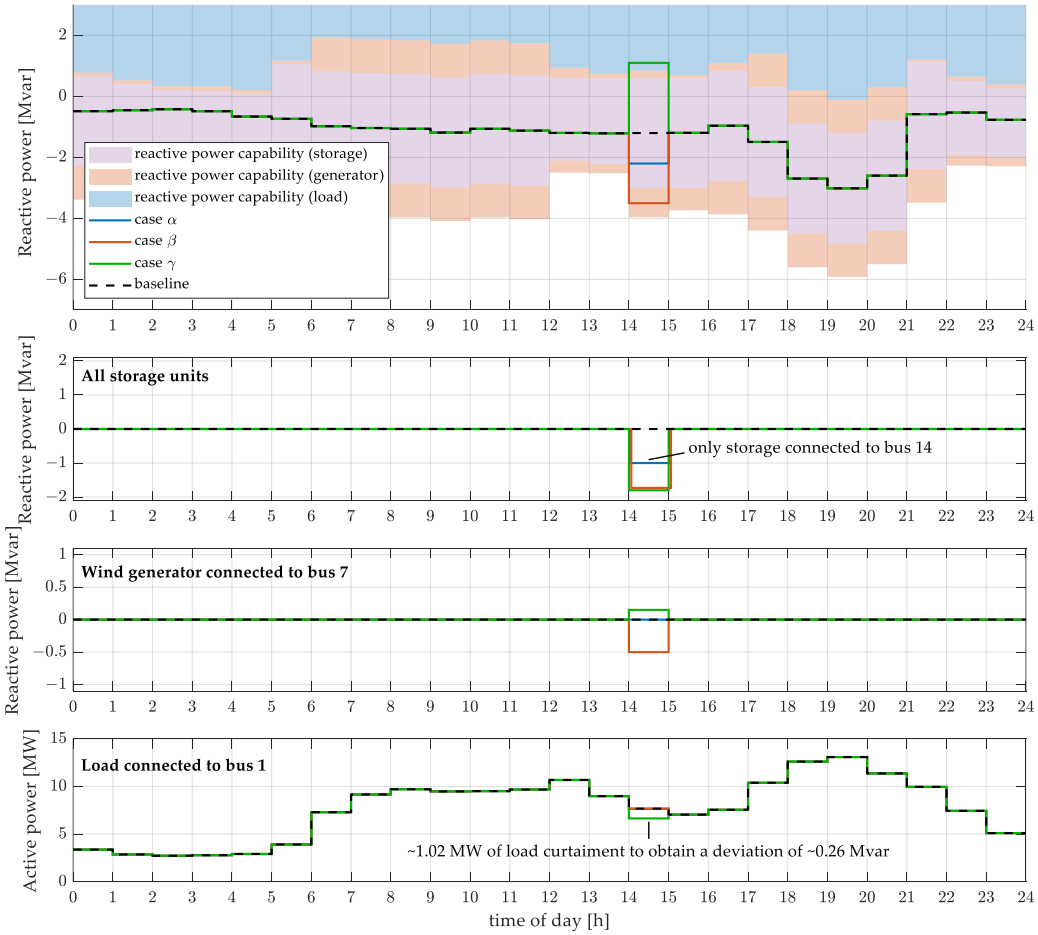


Figure 31. Total and individual reactive power exchange of storage, generation, and load units in cases α, β, and γ. S-DN1 is used to analyze the distribution network behavior during post-contingency hours (case A1, contingency 31). Load variation is represented by using active power, based on the observed power factor of 0.97.

5. Conclusions

This paper has introduced a novel surrogate modeling approach for representing the aggregated flexibility of distribution networks, specifically designed to facilitate the integration of distributed resources into transmission-level optimization and resilience frameworks. The surrogate model, composed of standard power flow elements (storage, generators, and loads), enables a compact yet accurate abstraction of the distribution network flexibility, ensuring compatibility with conventional OPF formulations and reducing computational complexity in transmission-level optimization tasks.

The methodology was demonstrated on a benchmark distribution network, where the step-by-step construction of each surrogate component was detailed and validated against the full network model. The results show that the surrogate model is able to capture the essential techno-economic characteristics and flexibility margins of the original system, with a good degree of correspondence under various operating conditions. While some approximation is inevitable, especially under severe network congestion, the surrogate model prioritizes feasibility and reliability of flexibility representations.

This paper has presented the integration of these proposed surrogate models in a framework for TSO-DSO coordination in order to improve the resilience in case of extreme events. Simulation results of the application of such a framework on a transmission and distribution test system demonstrate that surrogate models are an effective interface for TSOs and DSOs to exchange information and model the flexibility of distribution networks.

The comparison of different simulation cases considering different costs for ancillary services and different operation modes of distribution network shows that utilizing its flexibility to support transmission resilience leads to lower costs and improved system performance (in terms of lower CVAR of Cost of Energy Not Served) compared to traditional emergency measures.

Overall, the proposed surrogate modeling approach offers a scalable and interoperable solution for integrating distribution-level flexibility into transmission system operations, with significant benefits for system resilience and cost efficiency. Future research will focus on extending the surrogate modeling framework to account for additional sources of flexibility, more complex network topologies, and real-time implementation aspects, as well as exploring its application in other ancillary service markets and regulatory contexts.

Author Contributions: Conceptualization, M.R. and G.V.; methodology, A.P., E.C., M.R. and G.V.; software, A.P. and M.R.; validation, A.P. and M.R.; formal analysis, A.P., E.C., M.R. and G.V.; investigation, A.P., E.C., M.R. and G.V.; data curation, A.P. and M.R.; writing—original draft preparation, A.P., E.C. and M.R.; writing—review and editing, A.P., E.C., M.R. and G.V. All authors have read and agreed to the published version of the manuscript.

Funding: This research was funded by the Research Fund for the Italian Electrical System under the Three-Year Research Plan 2025–2027 (MASE, Decree n. 388 of 6 November 2024), in compliance with the Decree of 12 April 2024.

Data Availability Statement: The raw data supporting the conclusions of this article will be made available by the authors on request.

Conflicts of Interest: Author Marco Rossi, Andrea Pitto, Emanuele Ciapessoni, Giacomo Viganò were employed by the company Ricerca sul Sistema Energetico (RSE s.p.a.). The remaining authors declare that the research was conducted in the absence of any commercial or financial relationships that could be construed as a potential conflict of interest.

References

1. Pilo, F.; Mauri, G.; Bak-Jensen, B.; Kampf, E.; Taylor, J.; Silvestro, F. Control and automation functions at the TSO and DSO interface—Impact on network planning. In Proceedings of the International Conference on Electricity Distribution, Galsgow, UK, 12–15 June 2017.
2. Pilo, F.; Mauri, G.; Hanlon, S.; Jupe, S.; Silvestro, F. Control and automation systems for electricity distribution networks of the future—An update on the activities of joint working group CIGRE C6.25/B5/CIRED. In Proceedings of the International Conference on Electricity Distribution, Lyon, France, 15–18 June 2015.
3. Kornrumpf, T.; Zdrallek, M.; Roch, M.; Salomon, D.; Pyro, P.; Hobus, I. Flexibility Options for Medium Voltage Grid Planning. In Proceedings of the International Conference on Electricity Distribution, Galsgow, UK, 12–15 June 2017.
4. Nguyen, H.; Kok, K.; Tran, T.T.; Nguyen, P.H. The Coordination Between TSO and DSO in the Context of Energy Transition—A Review. In Proceedings of the International Universities Power Engineering Conference, Cardiff, UK, 2–6 September 2024.
5. Couto, M.; Javadi, M.S.; Osório, G.J.; Catalão, J.P.S. Global Perspectives on Tso-Dso Coordination Models for Distributed Energy Resources Market Integration. In Proceedings of the International Conference on the European Energy Market, Lisbon, France, 27–29 May 2025.
6. Viganò, G.; Lattanzio, G.; Rossi, M. Review of Main Projects, Characteristics and Challenges in Flexibility Markets for Services Addressed to Electricity Distribution Network. *Energies* **2024**, *17*, 2781. [CrossRef]
7. Silvestro, F.; Pilo, F.; Araneda, J.C.; Braun, M.; Taylor, J.; Alvarez-Herault, M.C.; Heymann, F. Review of Transmission and Distribution Investment Decision Making Processes under increasing Energy Scenario Uncertainty. In Proceedings of the International Conference on Electricity Distribution, Madrid, Spain, 3–6 June 2019.
8. Joint Working Group CIGRE/CIRED C1.29. Planning Criteria for Future Transmission Networks in the Presence of a Greater Variability of Power Exchange with Distribution Systems. 2017.
9. EPRI. *Developing a Framework for Integrated Energy Network Planning (IEN-P)*; EPRI: Palo Alto, CA, USA, 2018.
10. Schaefer, F.; Menke, J.; Marten, F.; Braun, M. Time Series Based Power System Planning Including Storage Systems and Curtailment Strategies. In Proceedings of the International Conference on Electricity Distribution, Madrid, Spain, 3–6 June 2019.

11. Jendernalik, L.; Giavarra, D.; Engels, C.; Hiry, J.; Kittl, C.; Rehtanz, C. A Holistic Network Planning Approach: Enhancement of the Grid Expansion using the Flexibility of Network participants. In Proceedings of the International Conference on Electricity Distribution, Galsgow, UK, 12–15 June 2017.
12. Bytyqi, A.; Gandhi, S.; Lambert, E.; Petrovič, N. A review on tso-dso data exchange, cim extensions and interoperability aspects. *J. Mod. Power Syst. Clean Energy* **2022**, *10*, 309–315. [CrossRef]
13. Zafeiropoulou, M.; Sijakovic, N.; Zarkovic, M.; Ristic, V.; Terzic, A.; Makrygiorgou, D.; Zoulias, E.; Vita, V.; Maris, T.I.; Fotis, G. Development and Implementation of a Flexibility Platform for Active System Management at Both Transmission and Distribution Level in Greece. *Appl. Sci.* **2023**, *13*, 11248. [CrossRef]
14. Papazoglou, G.; Biskas, P. Review of Methodologies for the Assessment of Feasible Operating Regions at the TSO–DSO Interface. *Energies* **2022**, *15*, 5147. [CrossRef]
15. Sarstedt, M.; Kluß, L.; Gerster, J.; Meldau, T.; Hofmann, L. Survey and Comparison of Optimization-Based Aggregation Methods for the Determination of the Flexibility Potentials at Vertical System Interconnections. *Energies* **2021**, *14*, 687. [CrossRef]
16. Riaz, S.; Mancarella, P. Modelling and Characterisation of Flexibility From Distributed Energy Resources. *IEEE Trans. Power Syst.* **2022**, *37*, 38–50. [CrossRef]
17. Lazaridou, G.E.; Sarafoglou, E.; Fesakis, N.; Boglou, V.; Karlis, A. A Critical Review on Flexibility Quantification and Evaluation Methods in Medium and Low Voltage Networks. *IEEE Access* **2025**, *13*, 92622–92640. [CrossRef]
18. Sarstedt, M.; Hofmann, L. Monetarization of the Feasible Operation Region of Active Distribution Grids Based on a Cost-Optimal Flexibility Disaggregation. *IEEE Access* **2022**, *10*, 5402–5415. [CrossRef]
19. Singhal, A.; Bharati, A.K.; Ajjarapu, V. Deriving DERs VAR-Capability Curve at TSO-DSO Interface to Provide Grid Services. *IEEE Trans. Power Syst.* **2023**, *38*, 1820–1833. [CrossRef]
20. Javed, A.H.; van der Holst, B.; Nguyen, P.H.; Morren, J.; Slootweg, J.G. Analyzing impact of network constraints on feasible operation region of the radial distribution networks. *Electr. Power Syst. Res.* **2024**, *234*, 110799. [CrossRef]
21. Zimmerman, R.D.; Murillo-Sanchez, C.E.; Thomas, R.J. MATPOWER: Steady-State Operations, Planning and Analysis Tools for Power Systems Research and Education. *IEEE Trans. Power Syst.* **2011**, *26*, 12–19. [CrossRef]
22. Rossini, M.; Rossi, M.; Siface, D. A surrogate Model of Distribution Networks to Support Transmission Network Planning. In Proceedings of the International Conference on Electricity Distribution, Rome, Italy, 12–15 June 2023.
23. CIGRE. Benchmark Systems for Network Integration of Renewable and Distributed Energy Resources. Available online: https://www.e-cigre.org/publications/detail/575-benchmark-systems-for-network-integration-of-renewable-and-distributed-energy-resources.html (accessed on 17 October 2025).
24. Rossi, M.; Viganò, G.; Moneta, D.; Vespucci, M.T.; Piscella, P. Fast estimation of equivalent capability for active distribution networks. *CIRED—Open Access Proc. J.* **2017**, *2017*, 1763–1767. [CrossRef]
25. Rossi, M.; Viganò, G.; Rossini, M. Linear optimal power flow model for modern distribution systems: Management of normally closed loop grids and on-load tap changers. *Electr. Power Syst. Res.* **2024**, *235*, 110653. [CrossRef]
26. Laoharojanaphand, V.; Ongsakul, W. Optimal Power Scheduling of Hydropower with Co-Located Floating Solar and Wind Generation Using Stochastic Weight Tradeoff Chaotic Particle Swarm Optimization. *Electr. Power Compon. Syst.* **2022**, *50*, 1223–1236. [CrossRef]
27. Roald, L.A.; Pozo, D.; Papavasiliou, A.; Molzahn, D.K.; Kazempour, J.; Conejo, A. Power systems optimization under uncertainty: A review of methods and applications. *Electr. Power Syst. Res.* **2023**, *214*, 108725. [CrossRef]
28. Uryasev, S.; Rockafellar, R.T. Conditional Value-at-Risk: Optimization Approach. In *Stochastic Optimization: Algorithms and Applications*, 1st ed.; Uryasev, S., Pardalos, P.M., Eds.; Springer Nature: Boston, MA, USA, 2001.
29. Pitto, A.; Ciapessoni, E.; Rossi, M.; Carlini, C. Methodology for Resilient Control and Coordination Between Interdependent Transmission and Distribution Networks. Available online: https://www.rse-web.it/en/reports/methodology-for-resilient-control-and-coordination-between-interdependent-transmission-and-distribution-networks/ (accessed on 17 October 2025).
30. Power Systems Test Case Archive. Available online: http://www.ee.washington.edu/research/pstca/ (accessed on 3 September 2025).
31. Pitto, A.; Ciapessoni, E.; Ferrario, E. New Vulnerability Models and Evaluation of the Effects of Uncertainties on Electric System Resilience Indices. Available online: https://www.rse-web.it/en/reports/vulnerability-models-of-the-electrical-system-even-in-the-presence-of-simultaneous-threats/ (accessed on 17 October 2025).

Disclaimer/Publisher's Note: The statements, opinions and data contained in all publications are solely those of the individual author(s) and contributor(s) and not of MDPI and/or the editor(s). MDPI and/or the editor(s) disclaim responsibility for any injury to people or property resulting from any ideas, methods, instructions or products referred to in the content.